

INVESTIGATION OF WEATHERING EFFECTS ON PERFORMANCE OF
INTUMESCENT COATINGS USED IN FIRE PROTECTION OF WOOD
STRUCTURES

by

Vahid Hemmati

A dissertation submitted to the faculty of
The University of North Carolina at Charlotte
in partial fulfillment of the requirements
for the degree of Doctor of Philosophy in
Mechanical Engineering

Charlotte

2017

Approved by:

Dr. Aixi Zhou

Dr. Russell Keanini

Dr. Stephen L. Quarles

Dr. Peter Tkacik

Dr. Mohammad A. Kazemi

ABSTRACT

VAHID HEMMATI. Investigation of Weathering Effects on Performance of Intumescent Coatings Used in Fire Protection of Wood Structures. (Under the direction of DR. AIXI ZHOU)

Intumescent coating is one of many passive methods to protect wood structures in the Wildland-Urban Interface (WUI) from fire. The intumescent coating forms a thick layer of carbonaceous char that protects the substrates from a fire attack. However, when the intumescent coating is used on the exterior of a structure, weathering may affect the process of the intumescent mechanism and the effectiveness of the coating. Also, coating chemicals under weathering effects may change into more ignitable substances and cause fire damage to the protected wood structure.

The purpose of this study was to investigate the weathering effect on the performance of the intumescent coating. There were two main concerns, the first concern was the possibility of decreasing ignition resistance of the coatings due to the weathering effect after a relatively short time. The second concern was the possibility of increasing the flammability of the coated specimens after weathering. To address these two concerns, the effects of weathering on the performance of fire retardant intumescent coating was studied. Calorimetry was used to collect the combustion data that formed 96 different classes of samples after various periods of natural weathering. The classes included samples that were exposed to the weathering effects for zero, three, six, and twelve months. Also, the samples were oriented northward and southward on the vertical weathering fence. Three different commercially available coating types were used to compare their performances to the weathering effects.

Then, randomly selected specimens from each class were tested in the cone calorimeter at three different heat flux levels. The data consisted of the following measured combustion properties; Time to Ignition (TTI), Heat Release Rate (HRR), Mass Loss Rate (MLR), and Effective Heat of Combustion (EHC). To measure these combustion properties, the cone calorimeter was employed. TTI, HRR and MLR are more important to address the first concerns. They can play an important role in ignition phase and propagation phase of a fire. However, EHC is the primary parameter that can be used to address the second concern of this study. If the intumescent coating materials were changed to a more combustible fuel (with higher EHC) than uncoated wood by natural weathering, it would be more reasonable to avoid using them as fire protection. In the next step, the ANOVA and MANOVA methods were employed as statistical tools to investigate the differences among the classes. Especially, the combustion properties were collected and compared for the 4 different weathering intervals to examine the effect of weathering on the two concerns. In addition, the machine learning method of Multi-class Decision Tree was employed to estimate the rank of each treatment effect on the response variables. The machine learning analysis showed that coating type is the most important factor in the ignition phase. TTI of samples was more affected by coating than the other involved parameters. However, in the propagation phase of fires, where HRR plays the major role, the weathering was the most effective factor. In the next step, the effects of weathering on all type of coated specimens were compared. In regards to the first concern: in almost all cases, the intumescent coatings showed a significant protection before weathering process. However, the fire protection decreased due to weathering, with an exception seen in

the weathering effects on EHC. The weathering process decreased the EHC in almost all cases. The degradation of the coatings was different by type. In the next stage, the performance of coated specimens was compared to uncoated counterparts. This comparison showed the advantage of each type in different weathering time intervals. In some cases, there is no statistical evidence of different performance between coated specimens than uncoated specimens in 12 months of weathering. In addressing the second concern, the increasing combustibility was not seen in the weathering process of the intumescent coating except in one case of HRR after 12 months of weathering. The most important factor related to the second concern was that EHC did not increase by weathering. In addition, the results showed that the water-based intumescent coatings with thicker coated layers displayed overall better performance (type C and A). From this result it could demonstrate that the physical properties such as thickness of the coatings may affect the life time of the coatings.

ACKNOWLEDGMENTS

This dissertation was not possible without the guidance, consideration and support of my advisor Dr. Aixi Zhou. His knowledgeable advising and friendly support provided motivation and friendly environment to conduct the research.

I, hereby, give my appreciation to Dr. Russell Keanini. I had the privilege of receiving his kind support since starting my Ph.D. program in 2013.

I would thank Dr. Stephen L. Quarles. He is a member of my committee and also senior scientist providing useful technical support in this project.

I am grateful to Dr. Peter Tkacik and Dr. Mohammad A. Kazemi, members of my committee, for their kind support.

I have to thank technical staff at the Insurance Institute for Business and Home Safety (IBHS) Research Center and the University of North Carolina at Charlotte for all their significant help.

My sincere thank goes to my friends and also colleagues, Babak Bahrani, Faraz Heydari, Jacob Kadel, and Gregorio Mesa.

I thank the Department of Mechanical Engineering and Engineering Science, The William Stats Lee collage of Engineering, Department of Engineering Technology and Construction Management and the Graduate School at the University of North Carolina at Charlotte, and the IBHS Research Center for providing financial and technical support for this research.

Contents

List of Figures	x
List of Tables.....	xii
CHAPTER 1. INTRODUCTION	1
1.1. Research Goal and procedure.....	1
1.2. Motivation	2
1.3. Objectives and Scope	4
1.4. Organization of Dissertation.....	4
CHAPTER 2. LITERATURE REVIEW	6
2.1. Introduction	6
2.2. Intumescent System.....	10
2.2.1. Intumescent Process and Optimization	12
2.3. Weathering Effect on Coatings	16
2.3.1. Weathering Technique	17
2.3.2. Weathering Effect Classification.....	19
2.3.3. Weathering Mechanisims of Degradation.....	20
2.3.4. Weathering Causes and Degradation.....	21
2.4. Effects of weathering on Performance of Intumescent Coating.....	25
2.5. Statistical Analysis	27
2.5.1. Theory of ANOVA.....	27

2.5.2. ANOVA in Practice.....	31
2.6. Heat Flux measurement in Fire Spread.....	32
2.7. Significance of Project	33
CHAPTER 3. RESEARCH METHODOLOGY	35
3.1. Preparation and Weathering	35
3.2. Measurement Apparatus.....	37
3.2.1. Cone Calorimeter	37
3.2.2. Oxygen Consumption Calorimetry Principles	38
3.2.3. Combustion Property in Calorimetry	39
3.3. Critical Heat Flux	41
3.4. Road Map of Project.....	44
CHAPTER 4: DATA ANALYSIS.....	50
4.1. Low Heat Flux Test.....	54
4.1.1. TTI in Low Heat Flux Test.....	54
4.1.2. HRR in Low Heat Flux Test.....	57
4.1.3. MLR in Low Heat Flux Test	59
4.1.4. EHC in Low Heat Flux Test.....	62
4.2. Medium Heat Flux Test.....	63
4.2.1. TTI in Medium Heat Flux Test	63
4.2.2. HRR in Medium Heat Flux Test	66

4.2.4. MLR in Medium Heat Flux Test.....	68
4.2.4. EHC in Medium Heat Flux Test.....	70
4.3. High Heat Flux Test	71
4.3.1. TTI in High Heat Flux Test.....	71
4.3.2. HRR in High Heat Flux Test.....	73
4.3.3. MLR in High Heat Flux Test	75
4.3.4. EHC in High Heat Flux Test	77
4.4. Overview of Coating Performance.....	78
4.4.1. Overview Over TTI of Coated Specimens	79
4.4.2. Overview Over HRR of Coated Specimens	80
4.4.3. Overview Over MLR of Coated Specimens.....	80
4.4.4. Overview Over EHC of Coated Specimens	81
4.4.5. Overview Over of Ignition Probablity.....	81
4.5. Critical Heat Flux	82
CHAPTER 5: CONCLUSION.....	84
5.1. Conclusion Results	84
5.2. Significant of Research.....	85
5.3. Recommendation for Future Reseach	86
BIBLOGRAPHY	88
APPENDIX: RAW DATA	98

List of Figures

FIGURE 1: Formation of charred layer (Picture by Babak Bahrani)	7
FIGURE 2: Example of main chemical stages in intumescent mechanism	8
FIGURE 3: Typical natural weathering testing rack	18
FIGURE 4: Weathering testing rack of this project	18
FIGURE 5: Beta scission reaction	20
FIGURE 6: Cross-linking polymers	21
FIGURE 7: Photo-oxidation in polymers	22
FIGURE 8: Probability density of F-factor	30
FIGURE 9: ANOVA table reported by MATLAB	31
FIGURE 10: Racks specification	36
FIGURE 11: Cone Calorimetry and control volume used in calculation of oxygen consumption	38
FIGURE 12: Thermally thick solid sample under constant heat flux	42
FIGURE 13: Method of measuring critical heat flux	43
FIGURE 14: Thermally thin solid sample under constant heat flux	44
FIGURE 15: Degree of freedoms in the weathering effect study	45
FIGURE 16: Flowchart to find effective treatments	47
FIGURE 17: Flowchart to investigate weathering effects	48
FIGURE 18: Flowchart to investigate coating effects	49
FIGURE 19: Predictor Importance for TTI	52
FIGURE 20: Predictor Importance for HRR	53
FIGURE 21: Effect of weathering on TTI in low heat flux test	55

FIGURE 22: Effect of weathering on HRR in low heat flux test	57
FIGURE 23: Effect of weathering on MLR in low heat flux test	60
FIGURE 24: Effect of weathering on EHC in low heat flux test	62
FIGURE 25: Effect of weathering on TTI in low heat flux test	64
FIGURE 26: Effect of weathering on HRR in medium heat flux test	66
FIGURE 27: Effect of weathering on MLR in medium heat flux test	68
FIGURE 28: Effect of weathering on EHC in medium heat flux test	70
FIGURE 29: Effect of weathering on MLR in medium heat flux test	72
FIGURE 30: Effect of weathering on HRR in high heat flux test	74
FIGURE 31: Effect of weathering on MLR in high heat flux test	76
FIGURE 32: Effect of weathering on EHC in high heat flux test	78
FIGURE 33: Effect of weathering on TTI	79
FIGURE 34: Effect of weathering on HRR	80
FIGURE 35: Effect of weathering on MLR	81

List of Tables

TABLE 1: Some materials commonly used in intumescent retardant coating	9
TABLE 2: Duration of heat fluxes in second for each category of low, medium and high heat flux.	33
TABLE 3: Coating system overview.	35
TABLE 4: Timetable of weathering process	37
TABLE 5: MANOVA results for all different treatments.	50
TABLE 6: P-values comparing performance of coated from uncoated counterparts in TTI under low heat flux.	56
TABLE 7: Change in average of TTI in second because of coating in low heat flux tests.	56
TABLE 8: P-values comparing performance of coated from uncoated counterparts in HRR under low heat flux.	58
TABLE 9: Change in average of HRR in kW/m^2 because of coating in low heat flux tests.	58
TABLE 10: P-values comparing performance of coated from uncoated counterparts in MLR under low heat flux.	61
TABLE 11: Change in average of MLR in $gr/s.m^2$ because of coating in low heat flux tests.	61
TABLE 12: Change in average of EHC in MJ/kg because of coating in low heat flux tests.	63
TABLE 13: P-values comparing performance of coated from uncoated counterparts in EHC under low heat flux.	63
TABLE 14: Change in average of TTI in second because of coating in medium heat flux tests.	65
TABLE 15: P-values comparing performance of coated from uncoated counterparts in TII under medium heat flux.	65

TABLE 16: Change in average of HRR in kW/m^2 because of coating in medium heat flux tests.	67
TABLE 17: P-values comparing performance of coated from uncoated counterparts in HRR under medium heat flux.	67
TABLE 18: Change in average of MLR in $gr/s.m^2$ because of coating in medium heat flux tests.	69
TABLE 19: P-values comparing performance of coated from uncoated counterparts in MLR under medium heat flux.	69
TABLE 20: Change in average of EHC in MJ/kg due to coating under medium heat flux tests.	71
TABLE 21: P-values comparing performance of coated from uncoated counterparts in EHC under medium heat flux.	71
TABLE 22: Change in average of TTI in second because of coating in high heat flux tests.	73
TABLE 23: P-values comparing performance of coated from uncoated counterparts in TTI under high heat flux.	73
TABLE 24: Change in average of HRR in kW/m^2 because of coating in high heat flux tests.	75
TABLE 25: P-values comparing performance of coated from uncoated counterparts in HRR under high heat flux.	75
TABLE 26: Change in average of MLR because of coating in high heat flux tests.	76
TABLE 27: P-values comparing performance of coated from uncoated counterparts in MLR under high heat flux.	77
TABLE 28: Change in average of EHC in MJ/kg because of coating in high heat flux tests.	78
TABLE 29: P-values comparing performance of coated from uncoated counterparts in EHC under high heat flux.	79
TABLE 30: Critical heat fluxes based on thermally thick solid model.	82

TABLE 31: Critical heat fluxes based on thermally thin solid model.

CHAPTER 1: INTRODUCTION

1.1 Research Goal and Procedure

The main goal of this research was to determine and investigate the weathering effects on the intumescent coating. Intumescent coatings have been applied to structures as protection for over 50 years, most recently applied to wood structures in the WUI. However, the performance of the intumescent coatings could be affected by weathering.

There were two major concerns which may challenge the advantage of using intumescent coating as a widely used passive fire protection in WUI fires. First, weathering may decrease the fire retardant efficiency of the intumescent coating in such a way that the coating does not offer sufficient protection until the end of the predicted service life. Second, the combustibility of the intumescent coatings may increase due to the chemical composition of the coatings being affected by the weathering conditions resulting in the coating to be more ignitable.

To address the concerns, this project was divided into four major tasks. In the first task, specimens were prepared, wood panels were cut into the appropriate size, and coatings were applied on the specimens. In the second task, the coated specimens were exposed to natural weathering. In the third task, the combustion properties of the samples were measured using the cone calorimeter. In the last task, the measured

combustion properties were statistically analyzed.

1.2 Motivation

WUI fires have caused a lot of damage and many casualties in human history. WUI consists of a geometric location where man-made structures and combustible natural fuel, such as vegetation, merge with the environment. Based on the fact sheet of the International Association of Wildland Fire (IAWF) published in August 2013, around 220 million acres in the United States are in high-risk zones. This area has been growing rapidly due to civil developments with the rate of two million acres per year since 1990.

The threat of WUI fire exists all over the United States, however, the risk is more serious in the west where the records show higher wildfire frequency. Two recent devastating fires can be considered as fires in the WUI: Wrightwood California USA on August 2016 and San Diego County fire in October 2003. On the other hand, human activities have made the wildfire more unpredictable, such as the Gatlinburg TN fire in Fall of 2016. Wildfires used to be more natural and seasonal. Now, every month of the calendar year, there is the risk of fire in WUI. Therefore fire protection in WUI is now a year-round obligation.

The increasing trend in the number of the structures and human lives lost in wildfires worries decision makers all over the world. The data by NIFC (National Interagency Fire Center) showed almost 10% increase in the loss rate of the structures in wildfires in the United States from the beginning of the century. The annual budget of over

\$4.7 billion in 2012 dedicated to controlling wildland fire shows the importance of the problem in the United States alone.

The possible solutions to mitigate fire damage to structures are classified in two major fire protection systems: Active Fire Protection Systems (AFPS) and Passive Fire Protection Systems (PFPS). AFPS are used to detect, control and extinguish fires by consuming energy and doing external work. Systems such as fire detectors, sprinklers, fire-engine belong to this category. On the other hand, PFPS do not require external work to protect structures. These systems work by their existence in the danger zone of fires. In application, the PFPS are mostly employed to delay ignition and slow down fire propagation. Systems such as fire dampers, fire doors and firewalls can be considered as PFPS. Treatments, such as using fire retardant materials or wetting agents also belong to this category.

One vital aspect of WUI fire is the speed of the fire propagation. A rapid temperature rising rate can challenge all the appropriate active firefighting measures. In that, the passive methods to control and suppress fire show their significance. The delay in ignition and propagation of fires enables firefighters to mobilize their efforts, save more lives, and structures.

One of the well-known PFPS is intumescent coating. Intumescent coating causes a delay in ignition by forming an intumescent layer. This mechanism works, however, weathering may affect the coating performance especially in external applications.

1.3 Objectives and Scope

The purpose of this study was to investigate the weathering effect on the performance of the intumescent coating. There were two main concerns, the first concern was the possibility of decreasing ignition resistance of the coatings due to the weathering effect after a relatively short time. The second concern was the possibility of increasing the flammability of the coated specimens after weathering. To address these two concerns, this project was constructed. The main tasks in this project to achieve the research goal were defined as follows;

First, the specimens were coated with three different coating types (A, B, and C), and one group was kept uncoated as a baseline.

Then, the specimens were exposed to natural weathering. In installing the specimens, two different orientations were selected; toward north and south. The weathering groups consisted of specimens exposed to natural weathering for zero, three, six, and twelve months.

In the third task, the combustion properties of specimens were tested using the Cone Calorimeter in three different heat flux levels (low, medium and high heat flux).

In the last task, the collected data was statistically studied using both analyses of variance (ANOVA) and multivariate analysis of variance (MANOVA) methods to determine the effects of weathering.

1.4 Organization of Dissertation

This dissertation consists of five chapters. First, in the introduction chapter, the research objective, the brief background, and the problem statement is explained.

The second chapter is dedicated to the literature review. The second chapter consists of reviewing the literature about five important topics: intumescent coating, the weathering effects on coating materials, the weathering effects on intumescent coating, effective heat flux measurement in fires and relevant statistical tools. At the end of the second chapter, knowledge gaps are discussed. In the third chapter, the research methodology is explained. This chapter explains the tasks that were done to achieve the objective. Analysis of variance (ANOVA and MANOVA) methods are the main focus of the third chapter. In the fourth chapter, the results of the statistical analysis are presented. Finally, the last chapter includes the conclusion and recommendations.

CHAPTER 2: LITERATURE REVIEW

2.1 Introduction

Fire protection systems consist of passive and active systems. Active Fire Protection Systems (AFPS) are mostly used at the time of incidents to manage or finally extinguish the fire through action. The main character of AFPS is their requirement of doing physical work in order to operate the systems. A wide range of systems from smoke/fire alarming systems to sprinklers and extinguishers are categorized as AFPS. Passive Fire Protection Systems (PFPS) do not require any physical work to operate at the time of a fire incident. These systems work simply by their existence in the incident scene such as fire walls, protection coating layers, and wetting agents. The used of noncombustible materials or fire-resistance materials in structures can be considered as PFPS. Intumescent coating is one of the PFPS used to protect structures. An intumescent coating treatment is not only relatively simple to apply, but also it is considered as an economic PFPS solution for the growing problem [1].

An intumescent system produces foam upon exposure to heat. The puffed up foam from the coating forms an insulating char layer covering all over the combustible materials like wood, plastic, or metals used in structures. This char layer causes a delay in ignition by protecting the flammable substrate from heat and oxygen.

As displayed in Figure 1, the intumescent char layer insulates the substrate from

heat and oxygen, the two elements required for combustion. This simple mechanism suffocates possible fire by depriving the fuel, substrate, from oxygen and heat, consequently, time to ignition increases. Most of the intumescent retardant coatings are made of three important elements; carbon donor, acid donor, and blowing agent.

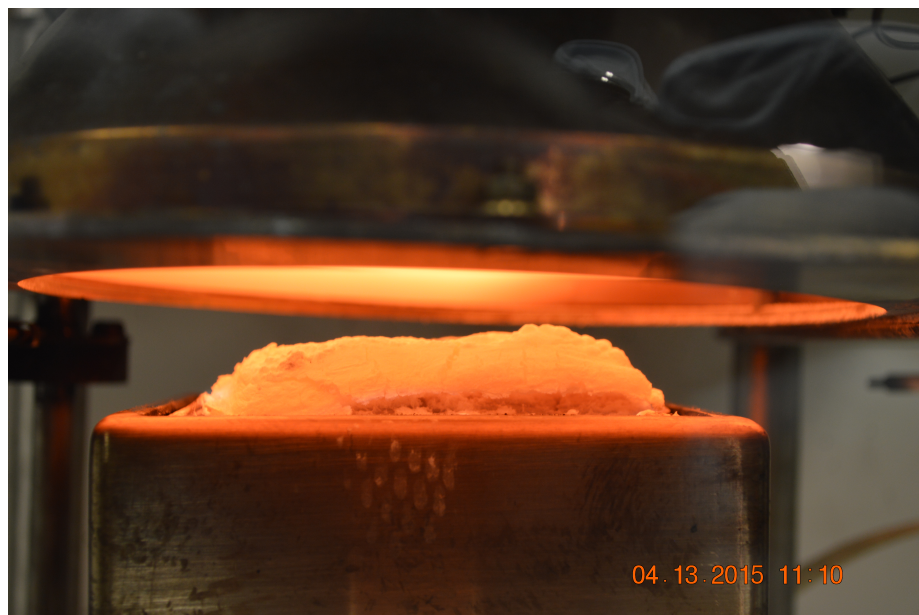


Figure 1: Formation of charred layer (Picture by Babak Bahrani)

Figure 2 shows an example of the chain of chemical reactions occurring in a popular intumescent coating (Phosphate-based system). As shown in this example, the chemical mechanism of an intumescent retardant coating can be simplified in three important stages. First, as a response to high temperature, an inorganic acid is released. It is the trigger of the system. In the case of Figure 2, the temperature must be higher than 250°C to activate the trigger. Ammonium Phosphate releases Meta-phosphoric Acid [2]. Then, in the second stage, Meta-phosphoric Acid in reaction with Polyalcohols provides char. The produced char works as the insulator

protecting the substrate from heat and oxygen. However, the protection would not be sufficient if the intumescent had not been formed. The last stage, in this simplified model, is the gas formation. The released gases, nitrogen and water vapor, force the char to swell up all over the substrate. The gas formation stage could play three important roles which cause delay to ignition. First, the swelled up char layer can cause increased distance between a substrate and the surrounding flame. This thick char layer acts like a thick thermal insulation. Second, the water as one of the products in the gas formation may cool up the substrates and adjacent space, therefore it takes a longer time to reach the critical temperature of protected substrates which cause a delay in ignition. The last role can be absorbing oxygen from the surrounding atmosphere which may decrease the chance of combustion. In the gas formation of the example shown in Figure 2, oxygen interacts with NH_3 and the results are nitrogen and vapor. This chemical reaction consumes the surrounding oxygen in the process of gas formation.

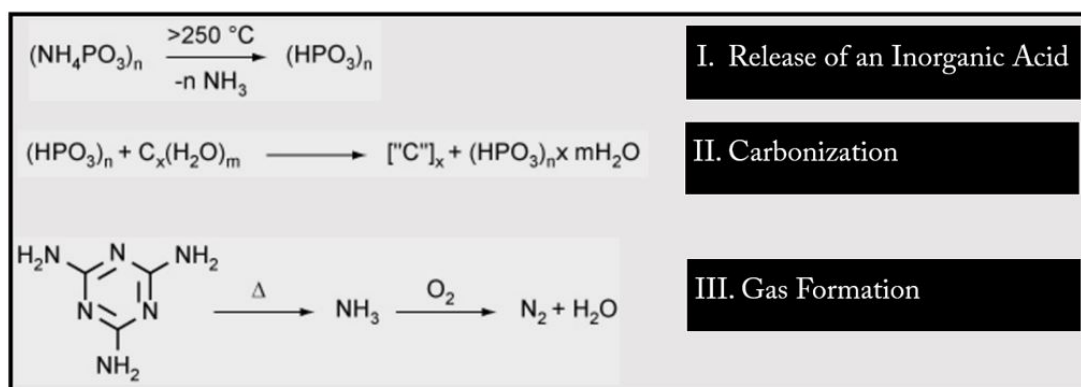


Figure 2: Example of main chemical stages in intumescent mechanism

The performance of an intumescent retardant coating is affected based on the type

Table 1: Some materials commonly used in intumescent retardant coating

<p>Acid Donors:</p> <ul style="list-style-type: none"> - Ammonium Salt - Phosphates of Amine or Amide - Organophosphorus Compounds <p>Carbon Donors:</p> <ul style="list-style-type: none"> - Starch - Dextrin - Sorbitol, Mannitol - Phenol-formaldehyde Resins - Charring Former Polymer - Pentaerythritol, Monomer, Dimer, Trimer - Methylol Melamine <p>Spumific (Blowing Agent):</p> <ul style="list-style-type: none"> - Amines/Amides - Melamine - Urea-Formaldehyde Resin - Polyamides - Dicyandiamide

and quality of the chemicals used as an acid donor, carbon donor and spumific. Each of these elements participates correspondingly in the acid releasing, carbonization and gas formation. The common materials used in intumescent retardant coatings are listed in Table (1) [1].

Intumescent coatings can be categorized into Epoxy-based and Acrylic-based [1]. The Epoxy-based intumescent coatings are mostly used for steel structures due to their resistance to corrosion. The Acrylic-based are classified in two main categories; water-based and solvent-based. The Acrylic-based coatings which solvable in water are more environment-

friendly, therefore, they can be used for interior applications. However, the water-based coatings may not last long in a humid area. On the other hand, the solvent-based (Oil-based) coatings, as the second category, are used for exterior applications due to their robust properties against weathering [1].

2.2 Intumescent System

The Latin word of “Intumescent” means swelling up due to heat [3]. The actual word carries out the concept of burning behavior of some substances. However, the intumescent systems are used to cause a delay in the ignition or even to protect materials against fire by forming a protective layer. The historical background of the intumescent mechanism was backed to Vandersall works in the 1970s [4]. The swelled up a layer of char protects the substrates against flame and heat [5]. The porous structure of the charred layer has a respectively poor thermal conductivity, which makes it a significant barrier against heat.

The process of intumescent layer formations starts when the temperature over the surface reaches a specific point. At this temperature, an endothermic chemical reaction is triggered by thermal energy. The products of this chemical reaction, or chain of chemical reactions, generally consist of a carbonaceous, a viscous liquid and also a gas. The trapped gas inside the viscous liquid forms bubbles. The foam, as the result, expands into a layer several times thicker than the coating layer. Then the solidification of the viscous liquid by heat forms a light, porous charred layer all over the surface [3, 6]. The performance of an intumescent coating is examined

based on specific standards. The suggested formulations are tested based on the UL-94 protocols [7]. The UL-94 is designed by Underwriter's Laboratories. The UL-94 classifies substances according to their flammability properties. Although, the protocol determines the standards for test parameters. It is important to mention that the conventional mechanism of intumescent coatings are not the only mechanism available. One of the interesting approaches is to synthesise one molecule acting as the acid source, the carbon source, and also the blowing agent [8]. The formulation of Toluidine Spirocyclic Pentaerythritol Bisphosphonate (TSPB) as one huge molecule displayed promising results as a fire retardant system. The LOI up to 26.5 vol.% and achieving the V0 rating based on UL-94 protocol were reported as the performance of TSPB. In addition, one of the best performance was reported for Expandable Graphite (EG) intumescent system [9, 10, 11]. The performance of LOI up to 40 vol.% for this system was reported.

2.2.1 Intumescent Process and Optimization

One of the popular research branches in intumescent systems is the optimization of the formulation. The performance of the intumescent significantly depends on the combination of the ingredients. Therefore, many research groups investigate the chemistry of materials to develop optimized coating substances. Most of these groups have focused on the carbonization process due to the importance of charred layer to protect the substrate [12, 13, 14, 15, 16]. The main ingredient of the carbonization is Pentaerythritol (PER). As an additive, Ammonium Poly-Phosphate (APP) is used as the main acid source in intumescent systems. The APP/PER shows the significant fire retardant properties [13, 17, 18, 19]. Based on the UL-94 protocol, this combination can be classified in V0 class. APP is the salt of polyphosphoric acid and ammonia. It has the chemical structure of $[NH_4PO_3]_n$. APP has two different crystal phases (APP-I and APP-II). The number of the chain elements in the first phase is relatively small (n around 1000). Two important parameters to evaluate the ingredients used in the intumescent system are thermal stability and water solubility. In most of the cases, APP is mixed with two different filling materials to form the intumescent system. APP can be added in polyolefin or polypropylene (PP)[3]. Most of the intumescent system is made of APP/PER/PP due to suitable performance in the thermal range from 180° C up to 270 °C. Formation of inorganic acid as the result of an endothermic reaction of APP is the first stage of the intumescent mechanism [20]. Then, the acid and PER interact at the temperature around 300 °C, and one of the results of this reaction is phosphocarbonaceous. Next, the blowing agent releases gas

due to decomposition. The final result would be a charred layer after solidification. The performance of the charred layer highly depends on the dynamic properties of the porous charred structure such as thermal conductivity and mechanical strength. The mechanical and physical properties of isolative charred layered were investigated by several research groups. In Russia, a structurometer ST-1 has been developed to determine the mechanical strength of the charred layer [21]. In this research, the breaking stress was measured for porous charred structure in the room temperature. The more recent research mostly focused on the measuring the breaking stress in higher temperature where the charred layer must work as isolating layer [22, 23, 24]. The heat conductivity of the charred layer in high temperature plays a crucial role in the performance of an intumescent system. The porous structure of charred layer and the high range of the working temperature are two main challenges to determine the thermal conductivity. Thermal conductivity of intumescent char was the object of many research groups [25, 26, 27, 28, 29, 30, 31]. Transient Plane Source (TPS) technique was one of the methods employed to investigate the thermal conductivity of charred layer [32]. In TPS technique, the sample is located in between the heat source and heat sensor. However, the technique is recommended for homogeneous samples in the range of thermal conductivity of 0.01-500 $[W/m.K]$.

The form and shape of the intumescent char contribute significantly to the mechanical and physical properties of the layer. Therefore, the morphology of intumescent char was studied using various microscopic techniques. Scanning Electron Microscope (SEM) was one of the popular apparatus [33]. The porous charred layer is highly brittle, which makes 3D imaging complex [34, 35].

Additive material to APP/PER such as melamine was reported to increase the time to ignition [19]. Another improvement was reported by adding polymer as a carbon source to APP [36, 37, 38, 39, 40, 41]. The additive polymer to APP showed a significant reduction in the exudation [41]. One of the important criteria to determine the efficiency of a fire protection system is the Limiting Oxygen Index (LOI). The LOI is the minimum of oxygen concentration required to ignite a polymer. The higher LOI shows more thermal stability and heat resistivity. LOI is measured by cone calorimetry. The cone calorimetry results reported that the performance of the mixture of polypropylene (PP), thermoplastic polyurethane (TPU), and ammonium polyphosphate (APP) highly depends on the concentration of TPU/PP [37, 38]. Although the more thermal stability of APP was reported by adding PA-6 [39]. PA-6 is a polymer with the chemical structure of $(C_6H_{11}NO)_n$. PA-6 could block the dynamic of the decomposed materials from APP and make the mixture more stable. The fire retardant materials, those are water resistant, would promise a better performance especially after weathering effects. Therefore, water solubility and exudation must be considered to manufacture a better fire retardant materials. Several research groups concentrated on synthesis of a more efficient carbon source with a better water resistivity [42, 43, 44, 45, 46, 47, 48]. The type of the carbon agents affected the peak heat release rate (PHRR) dramatically. In one optimized formula (APP/MPyP/BSPPO corresponding ratio of 7:4:4), the reduction to 0.1 of its original PHRR was reported [3]. Adding Synergistic agents to APP is examined as a chemical treatment to achieve a better fire protection system. In chemistry, there can be Synergistic effects in the combination of materials. In a Synergistic system

of substances, the effect of the combination is higher than the sum of the individual effects of all the substances. The high thermal stabilities and improved charred structures were reported due to adding the synergistic substances. The formed charred layers in the presence of synergistic additives depicted stronger mechanical resistance, higher integrity, more homogeneity and denser structure [49, 50, 51, 52, 53]. Other improvements in the performance of the intumescent systems were aiming to reduce the water solubility [54, 55]. The sol-gel method was one of these improvements. The silicon oxide gel was used as water resistance coating all over the surface [54]. The 85% improvement in water solubility for the intumescent system was reported by using sol-gel treatment. The other protective factors such as LOI also were improved by sol-gel method using silicon oxide [56]. The better efficiency by employing the sol-gel method was reported in specimens with different water containing [56]. The results of the research suggests using the sol-gel method, especially in humid weather, after testing the immersed specimens in water for different time intervals.

Another category of the intumescent systems is the Melamine Phosphate (MP) category. The MP/PER formulation is one of the popular combination for intumescent in this category [57]. MP-based intumescent is more used in higher temperature due to the thermal stability of the ingredients [58]. The chemical mechanism of the MP-based intumescent is more complex, however, the principle of the forming a protective charred layer is still valid for MP systems.

The effect of the ingredients, MPP (MP/PER) GF-PA6.6 (glass reinforced PA6.6), on the UL-94 rating and LOI was investigated by several research teams [59, 60, 61, 62]. The researchers showed that the LOI grows up by increasing the weight percent-

age of MPP. The higher rate of increasing LOI was reported in the MPP content of around 25%. Just similar to APP-based intumescent, the synergistic agent was used to improve the protective property of MP-based intumescent [63, 64, 65].

Non-phosphorous system (such as ethylene-acrylate copolymer (EBA), silicone elastomer, and chalk) performance was investigated to find an optimum formulation [66, 67, 68]. The best performance of LOI up to 30 vol.% has been reported [68]. Two other important quantities were measured to compare the performances of the intumescent system in the different formulations. Time to ignite (TTI) and the peak heat release rate (PHRR) at the heat flux of 35 $[kW/m^2]$ were reported. PHRR of 326 $[kW/m^2]$ and the TTI of 148 $[s]$ were the optimized results measured for the intumescent system with the formulation of CaSiEBA.

2.3 Weathering Effect on Coating

The weathering effects on the materials consist of physical, chemical and biological effects. Water, wind, ice, sunshine, or even bacteria in nature can cause or accelerate changing in materials properties. Thermal stress, mechanical stress, dissolution, carbonization, hydration, oxidation are only some of the phenomena that materials in nature are exposed to. The weathering effects depend on the geography of the location. The humidity/dryness rate, sunshine/wind strength, existence of sand/salt in the surrounding environment, and other geographical factors involve in materials changing. In addition, the orientation of materials to the respect of the sun may affect the rate of material change. Another important factor by weathering in seasons. Ma-

terials were exposed to different weathering effects in different seasons, therefore their response to weather must be different. The complexity of weathering effects due to diversity of the natural causes makes simulation of such a system in the laboratories almost impossible.

Among all the natural weathering, the effects of moisture, ultraviolet radiation, temperature and temperature fluctuation on the polymer degradation were more investigated to produce premiere materials. The weathering effects on materials, especially polymers, consists the matter of interests for many research teams. This topic would be one of the main subject studied in more details in this chapter.

2.3.1 Weathering Technique

There are several techniques to examine the weathering effects. natural, accelerated natural and artificial weathering are the most used testing techniques.

During a natural weathering exposure, the specimens are placed in an exterior location for several months or years. In most of the cases, the inclined racks are used to hold the samples in a specific orientation. As shown in Figure 3, in some cases where the effect of solar radiation is investigated, a 45 degree angle toward the south in Northern hemisphere is used to receive the maximum solar radiation [ASTM D1014 (45 ° North)].

In our case, the samples were installed on a vertical wall, shown in Figure 4. The orientation of sample installation is important in vertical racks. Therefore the orientations toward south or north were considered as different treatments in statistical analysis for this project.

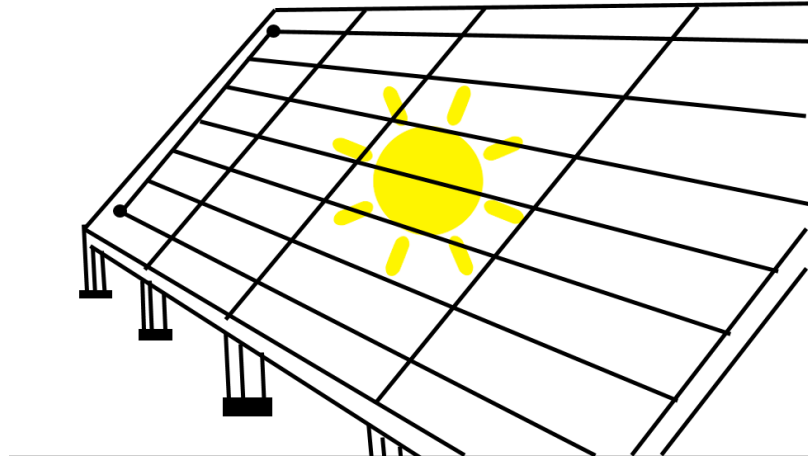


Figure 3: Typical natural weathering testing rack

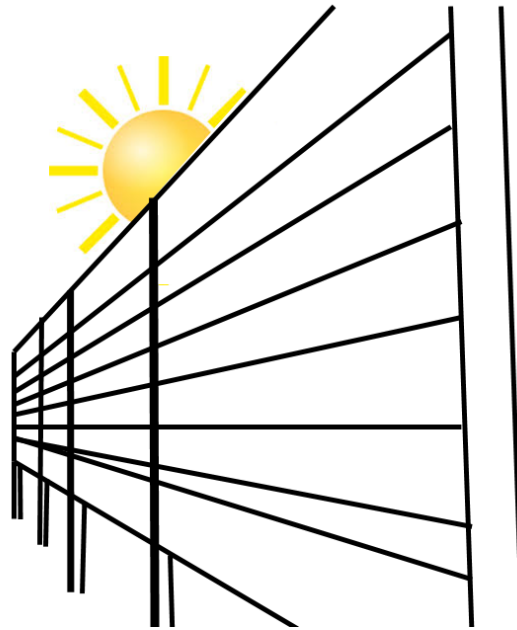


Figure 4: Weathering testing rack of this project

Another weathering technique is Accelerated Natural Weathering (ANW). In this technique, the natural effects are intensified by using apparatuses. The mirror can be used to focus the solar radiation on samples, or the inclined angle can be justified to maximize the cross-section along the winds. These techniques are employed to save

time. The effects of more than 60 years of UV radiation can be investigated in only one year by employing advanced ANW method [*ASTM STANDARD B117*].

The third technique is artificial weathering. An environmental chamber is one of the popular instruments used in this technique. To save time, the conditions inside these chambers are set to be more extreme than the real weathering conditions. In addition, the desirable weathering condition can be preserved in these chambers non-stop for several weeks [69].

2.3.2 Weathering Effect Classification

The weathering effects can be classified into two categories. The first category is Physical weathering or Mechanical weathering. In the physical weathering, the chemical structure of the polymer is not changed. The material may break into pieces or crack on the surface, however, the chemical structure is preserved. The physical weathering can destroy the fire protection properties of the coating due to peeling process.

The second category in weathering is biogeochemical weathering. In a biogeochemical degradation, the substances are changed in transferring between organic and environmental causes. This type of weathering changes the chemical structure of the polymers. In the case of the intumescent system, the biogeochemical weathering can deteriorate the effective ingredients of the system and consequently the fire protection could not be performed appropriately.

These two types of weathering effects coexist in the most of the weathering cases

found in nature.

2.3.3 Weathering Mechanisms of Degradation

The main chemical degradations due to natural weathering consist of chain scission, cross-link, and substitution reactions.

The chain scission, shown in Figure 5, is a thermal degradation when the polymer chains break down into smaller segments and these segments react with one another.

This reaction occurs in the absence of any chemical agent.

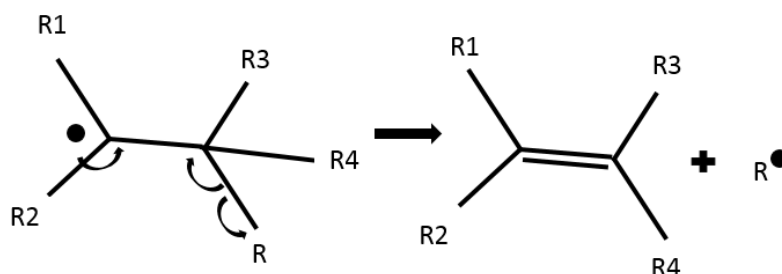


Figure 5: Beta scission reaction

The cross-link reaction, shown in Figure 6, is the formation of chemical bond between two polymer chains. The bonds in cross-link can be covalent or ionic bonds. The result of cross-link reaction could be a new polymer with different combustion properties.

The substitution reaction occurs when a group of chemical elements in the polymer is replaced by another group. This reaction required the existence a functional group of chemical in the environment.

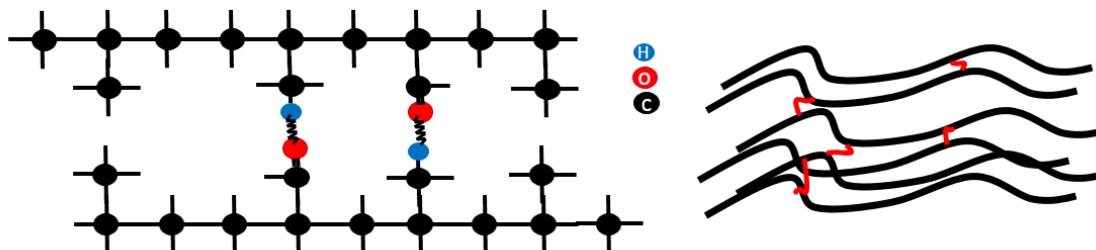


Figure 6: Cross-linking polymers

2.3.4 Weathering Causes and Degradation

Research on weathering effects on polymer degradations showed that the scission and cross-link occur more frequently than the substitution reaction.

Photo-oxidation, shown in Figure 7, thermal decomposition and oxidation, hydrolysis and pollutants attacks were reported as the major weathering effects on polymers.

The photo-oxidation can be the result of the photo collision and the presence of an impurity in polymer [70]. The photo-oxidation reactions can occur in darkness, however, the photo collision with sufficient energy can speed up the reaction [71]. The sufficient energy of the photon can be found in the radiation with a wavelength below 360 [nm] which categorized this spectrum in the ultraviolet range of radiation [71]. The final effect of the photo-oxidation on the polymer structure can be classified as chain scission. In some research, the effect of γ -radiation on the degradation of a polymer was investigated. The result showed the temperature had a significant influence on the effectiveness of γ -radiation in polymer degradation [72].

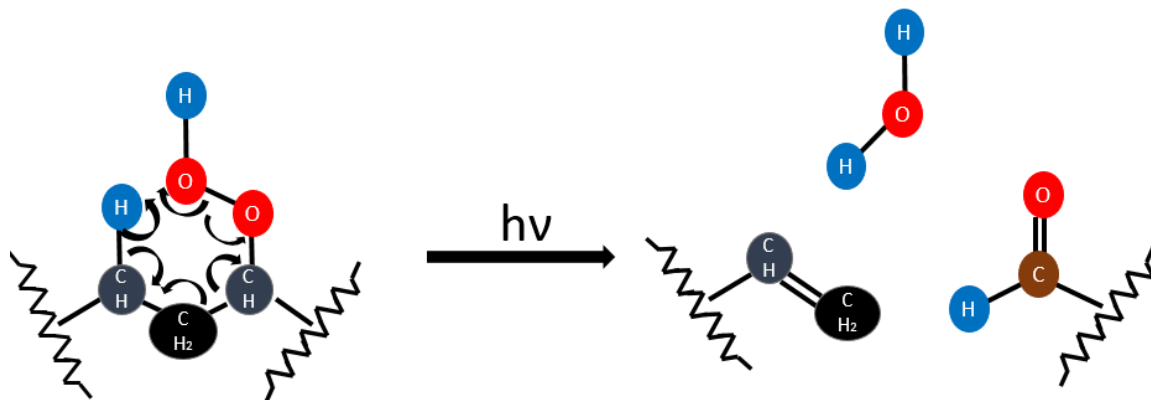


Figure 7: Photo-oxidation in polymers

Thermal decomposition and oxidation are serious degradations due to weathering. In most of the cases, the thermal decomposition and photo-oxidation coexist. The oxidation depends on both temperature and oxygen concentration. In a low amount of oxygen, the reaction occurs in higher temperature [73]. Formation of unstable fragments is the result of thermal degradation [74].

Hydrolysis results in the deterioration of properties of polymers through chain scission. The mechanical properties of the polymer are highly affected by hydrolysis. In some cases, the hydrolysis and water absorption occur simultaneously. Young's modulus may significantly decrease as result of both hydrolysis and water absorption [75]. This mechanism in the case of intumescent coating can lead to peeling off the protective layer.

Pollutants were investigated as a destructive factor for the chemical structure of polymer [76]. Pollutants, which are considered as a weathering factor, are the results

of human activities. Acid rains, formed by sulfur dioxide in the atmosphere, can wash off the intumescent coating from the surface of structures.

Mechanical degradation, due to thermal fluctuation, is another type of damage that can occur in the polymer structure. Thermal fluctuation could impose high stress upon materials. Sufficient stresses can break down the long chain of polymers. It is possible that segments of broken chain may not be able to rebound in the correct alignment. The mechanical-chemical degradation in rubber was investigated as a deteriorative phenomenon for decay [77]. In a case of the permanent and even weaker stresses, the chemical degradation rate increased [78]. Researchers displayed that the polymer having shorter molecular chain length with strained bonds degrade faster under the low stresses imposed by weathering [79, 80]. Another aspect of determining the strength of polymers against weathering is the chain orientation of the polymers. The highly oriented polymers share a load of stresses more evenly than the randomly oriented polymers, therefore they may last longer under weathering stresses [81]. Although, it is argued that the oxygen molecules have less chance to interact with the highly oriented polymer due to inaccessibility of weak part of bonds in the structure. Therefore, oxidation occurs more slowly in the high oriented polymers[78]. However, recent studies demonstrated that highly oriented PVC deteriorate faster due to photodegradation.

The lifetime of polymer, r , under the stress, σ , can be calculated by using the Zhurkov equation[82].

$$r = A \exp\left(\frac{\Delta G - B \sigma}{R T}\right) \quad (1)$$

where T is the temperature and the other parameters are constants. It is clear from the Zhurkov equation that the life time a typical polymer decreases exponentially by applying stress. The source of the stress can be weathering. The validity of the Zhurkov equation was confirmed by the Bueche's work [83]. The main challenge in the Zhurkov equation is to find a method to derive the unknown constants A and B.

There are several stress mechanisms in nature. Thermal fluctuation, chemical reaction, water absorption/desorption and secondary crystallization were discussed as the weathering mechanisms of imposing stress on polymers.

One interesting discovery was the ability of a chemical reaction to generate local stress. It is reported that oxidation could impose local stresses and these stresses mutually impressed the rate of the oxidation [78].

One of the weathering mechanism of apply stress on materials is through the water absorption/desorption process in nature [84, 85, 86, 87, 88]. Another source of stress on the materials by weathering is the secondary crystallization [89, 90].

The thermal fluctuation could affect the morphology of polymers. The morphology of a polymer is one of the important factors determining the rate of chemical reaction especially reaction with oxygen. Crystal phase, amorphous phase, and crystal-amorphous boundary phase behave differently toward the chemical reaction. The

degradation occurs mostly in an amorphous phase where the oxygen molecules could access to the weak joints in polymers structures[91].

2.4 Effects Of Weathering On Performance Of Intumescent Coating

Two important factors to rank intumescent coating are combustion properties and durability. Different ingredients depicted different performances. In most of the cases, the durability of a coating was checked only by investigating the effects of moisture in many coating types. In the more comprehensive investigation, which is more similar to the real application, the weathering must be considered. Long-term weathering effects on intumescent coating used for protection of wooden structure were studied in limited researches. One of the comprehensive studies was conducted by Babak Bahrani [1]. In this study, thermal decomposition tests and thermogravimetric analysis were performed. The results confirmed the effectiveness of intumescent coating to establish fire protection for wood before weathering. Also, the variance in combustion properties due to weathering such as TTI was reported. The heat flux level in the cone calorimetry tests was another important factor which was reported effective on the combustion properties of specimens. He reported that the orientation of installation did not cause a clear difference in performance of the weathered specimens. This project provided valuable data to study the natural weathering effects on intumescent coatings. The statistical analysis of this data would be the next step to understand the natural weathering on this type of FR coatings.

The effects of weathering on fire retardant intumescent were studied by other research teams. In the most of the cases, the type of intumescent which used to protect the

steel structures (epoxy based intumescent) were studied [92, 93]. In our case, the intumescent coating were water-base and it is expected to be affected differently from the epoxy base used for protection of steel structures.

The effects of natural weathering are relatively slow phenomena. It requires a long exposure time to observe the changes due to weathering. Therefore, researchers mostly preferred to save time by using the artificial or accelerated weathering techniques [92, 94].

The studies on weathering effects on fire retardant materials also included the impregnation treatment [95]. The impregnation treatment is not as simple as an intumescent coating in applications. This fact relatively limits the application of impregnation treatments in compared to coating treatments for already-built wooden structures.

The effects of artificial weathering on intumescent flame-retarded were studied by Almeras and colleagues [96]. The intumescent used in the study was ammonium polyphosphate (APP)/polyamide-6 (PA-6)/polypropylene(PP). The cone calorimetry detected the decreasing in the protection due to artificial weathering. The chemical degradation and morphological change (mechanical change) of APP were reported. The main degradation, reported in this study, was APP degradation into short chain of polyphosphates due to artificial weathering.

The studying on the effects of weathering on passive fire protection (PFP) used in offshore industries, especially oil and petrochemical industries conducted by Roberts and colleagues [97]. Steel is the main material which must be protected by PFP methods. In this study the long-term effects of weathering on six different epoxy base PFP systems were investigated. The effect of natural weathering changed based on

the roughness of the protected surface. The physical degradations were reported as one of main weathering effects on the tested PFP systems.

Another interesting aspect in the effects of natural weathering on FR material is the biological mechanism in degradation intumescent coatings. Many FR compositions contain materials which are nutrition sources for fungi [98]. The fungi grow can accelerate the weathering degradation of FR protection. In this study, several FR systems were investigated. The weathering effects on combustion properties and fungal decay were studied. The results showed the best performance in wood-plastic composites including expandable graphite treatments.

2.5 Statistical Analysis

The method, used to analyze the measured data, was the Analysis of Variable (ANOVA and MANOVA). This method is used to investigate the effectiveness of experimental treatments. The implementation of these methods to study weathering effect on intumescent coating sounds promising regarding the set up of the research.

2.5.1 Theory of ANOVA

Analysis of variance (ANOVA) is classified as one of the statistical hypothesis testing mostly employed in analyzing experimental data. This model is used to check difference among group averages when the sample size is much smaller than the population of groups.

Laplace was one of the pioneers in hypotheses testing. Also, Gauss is another mathematician who has a great contribution. These two mathematicians have developed a method for combining observation which can be considered as one of the oldest

versions of hypotheses testing method in statistic.

In 1918, Sir Ronald Aylmer Fisher, the British biologist, and mathematician published a research of the formal analysis, the term of the analysis of variance was mentioned for the first time in that article [99].

The main application of ANOVA method is when several random groups selected from the same population, then each group has been treated differently, and again some randomly picked up members of each group tested. The result of the test may be affected by the different treatment. ANOVA method provides statistical evidence of comparing the effectiveness of each treatment. The main challenge is the limit of the number of samples. Therefore the proof of the hypotheses that the response of different treatment ends up to different results in average, is not a trivial job.

There are a few assumptions in one way ANOVA. The distribution function considered for groups are assumed to be normal distributions with equal variance and independent errors [100].

The one way ANOVA evaluates the null hypothesis. The null hypothesis states that the means of all populations are equal. The alternative hypothesis says that at least the mean value of one of the populations differs from the other means.

The main equation in the one way ANOVA is the Fundamental ANOVA Identity equation.

$$\sum_{i=1}^k \sum_{j=1}^{n_i} (Y_{ij} - \bar{Y})^2 = \sum_{i=1}^k n_i (\bar{Y}_i - \bar{Y})^2 + \sum_{i=1}^k \sum_{j=1}^{n_i} (Y_{ij} - \bar{Y}_i)^2 \quad (2)$$

In the Fundamental ANOVA Identity equation (2), there are the following elements:

Y_{ij} is the element number j in the group number i .

\bar{Y} is the global average.

n_i is the population of group i .

\bar{Y}_i is the mean value of the group i .

The left side of the equation (2) is the square of the sum of deviations of all elements from the global average value. This term, $\sum_{i=1}^k \sum_{j=1}^{n_i} (Y_{ij} - \bar{Y})^2$, is called the Sum of Squares for total (SS_{total}).

The first term in the right side of the equation (2) is the square of the sum of the deviations of the mean of each group from the global average value. This term is multiplied to the population of each group. This term, $\sum_{i=1}^k n_i (\bar{Y}_i - \bar{Y})^2$, is called Sum of Squares for Treatment (SST).

The last term in right side of the equation (2) is in group calculation of the sum of the squares of the deviations of members of group from the average value of the group. This summation includes all groups. This term, $\sum_{i=1}^k \sum_{j=1}^{n_i} (Y_{ij} - \bar{Y}_i)^2$, is called Sum of Squares for Errors (SSE).

The Fundamental ANOVA Identity, the equation (2), can be summarized to the following equation.

$$SS_{total} = SST + SSE \quad (3)$$

F-factor is defined as the ratio of the variance between groups over the variance within the groups. Based on the definition SST and SSE, to have the required variances, theses values must be divided by the degree of freedom.

$$F = \frac{(\sum_{i=1}^k n_i (\bar{Y}_i - \bar{Y})^2) / (k - 1)}{(\sum_{i=1}^k \sum_{j=1}^{n_i} (Y_{ij} - \bar{Y}_i)^2) / (N - k)} = \frac{SST / (k - 1)}{SSE / (N - k)} \quad (4)$$

The higher F-factor shows the difference between groups are much bigger than the variance or difference within groups, therefore the null hypothesis is less probable to stay valid. In statistic, it is conventional to determine the certainty of assumptions by using distribution functions. In most of the cases, an assumption with the certainty above 95% is accepted as a valid assumption. The distribution function of F-factor is not a normal distribution anymore. Although, the degree of freedoms of a system, number of groups and population of the sample set, play a crucial role to determine the certainty using distribution function of F-factor. Another important parameter, in the one-way ANOVA method, is the P-value. The P-value shows the certainty in rejecting or accepting the null hypothesis.

The darker area beneath the curve, shown in Figure 8, is the confident area of the

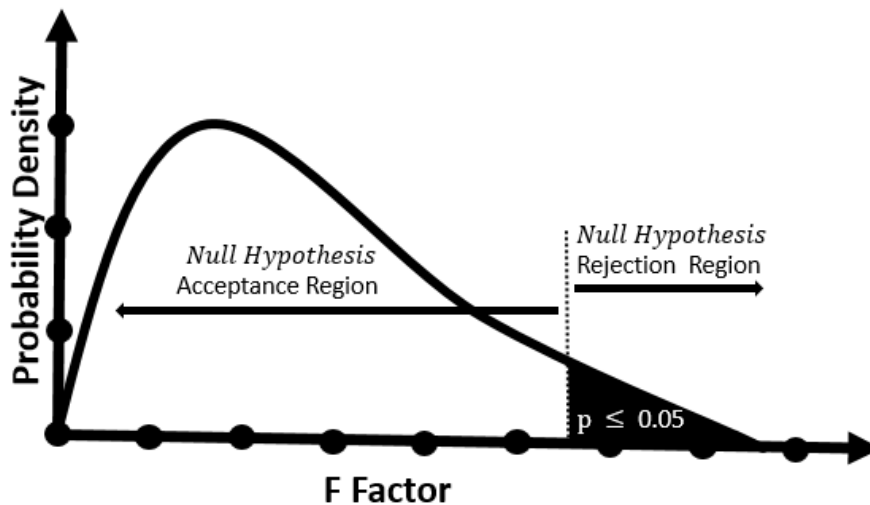


Figure 8: Probability density of F-factor

validity of the alternative hypothesis with more than 95% certainty. The distribution function curve is a function of the degree of freedom. It is conventional to accept the alternative hypothesis if F-factor belongs to this area.

2.5.2 ANOVA in Practice

One way ANOVA is a popular method in many scientific and engineering fields. In most of the cases, ANOVA method is implied to study the effectiveness of a specific treatment. The effectiveness of a suggested treatment is expected to shift the mean value of response variable in the randomly picked up sample set from entire population.

In this research, the intumescent coating was suggested as a treatment to improve fire protection properties of wood and wood-based application used in exterior applications. The fire protection properties, called the response variables in ANOVA terminology, consisted of TTI, HRR, the peak of HRR, MLR, and EHC. Weathering was considered as a treatment. This treatment can affect the response variables in a positive or negative way or have no effect. One way ANOVA was selected as the best statistical tool to detect the effects of weather on the performance of the intumescent coatings.

MATLAB has a subroutine for one-way ANOVA. In fact, ANOVA subroutines are available in most of the computer coding languages. The MATLAB subroutine that used in this research performed ANOVA and also Box-Plots is shown in ??.

All parameters which calculated in ANOVA are listed in output table of MATLAB

Source	SS	df	MS	F	Prob>F
Columns	75044.7	2	37522.3	33.77	0.0005
Error	6667.3	6	1111.2		
Total	81712	8			

Figure 9: ANOVA table reported by MATLAB

subroutine, shown in Figure 9. The second column in the table consists of SST , SSE ,

and SS_{total} . In the third column, the degree of freedoms is listed. In this column the first element comes from a number of the group $(k - 1)$, second element comes from sample population subtracted by the number of groups $(N - k)$, and the last element shows the degree of freedom comes from the sample size $(N - 1)$. The fourth column shows $SST/(k - 1)$ and $SSE/(N - k)$. F-factor is shown in the fifth column. Based on the degree of freedom and calculated F-factor, the MATLAB code determined the P-value from the available database. For P-values less than 0.05, the null hypothesis is rejected, and we are allowed to claim that at least the average value of one of the groups is different from the average values of the other groups.

2.6 Heat Flux Measurement in Fire Spread

As mentioned, three different heat flux levels (low, medium and high heat flux) were used in cone calorimetry tests for this project. In fact, the combustion properties could depend on the effective heat flux from cone. In real fire, wooden structures may be exposed to different level of heat fluxes. Temperature and heat flux measurement in wildland fires were conducted by Xavier Silvani and colleagues in France [101]. They used thermocouples and heat flux gauges in their experiments in wildland fires. Their report included both measurements of radiant and total heat fluxes. The data covered three stages of preheating, flaming, and charring of natural fuels in wildland fires. Their devices were installed on the top of vegetation. For such a device setup, they reported that radiation played the main role of heat transfer in fire propagations. Their results showed the duration of each heat flux level in second. Based on the

research, the Table (2) shows the extracted durations for the three heat flux levels used in cone calorimeter. The maximum duration for each category is shown in bold font. The exposure to low heat flux has the longest duration. The interesting result of very short duration of high heat flux in fires may reduce the relevant importance of studying the combustion properties of samples in this level in compare with medium and low heat flux tests.

Table 2: Duration of heat fluxes in second for each category of low, medium and high heat flux.

Heat Flux Level	Experiment 1	Experiment 2	Experiment 3	Experiment 4
Low (30 kW/m^2)	25 s	25 s	145 s	40 s
Meduim (50 kW/m^2)	0 s	0 s	60 s	10 s
High (70 kW/m^2)	0 s	0 s	5 s	8 s

2.7 Significance of Project

The artificial weathering were used by many research teams. The artificial weathering technique is not as time consuming as natural weathering, however, it is not comprehensive as natural weathering. As an example, in many artificial weathering the biological mechanism of degradation was not included.

In addition, most of research teams concentrated on PFP used in industries. Most of financial support in their researches came from oil and gas industries. The protection of steel structures against possible fires is the first priority for these companies. Therefore, most of researches concentrate on PFP for steel structures with epoxy bases.

There are researches on the natural weathering effects on intumescent coating used for protection wood structures. However, the lack of comprehensive statistical anal-

ysis was seen in many cases.

Despite many interesting types of research, there are few researches on the weathering effects on the performance of the intumescent coating with using the natural weathering. In this dissertation, the statistical techniques known as data mining provided a new approach to investigate the effectiveness of the weathering. In this method, the importance of the involved parameters can be ranked from most effective to the least based on combustion properties.

In addition, this study mostly concentrates on the real application where it is the possibility that the weathering disables the protection. Therefore, the results regardless of explanation in details can provide applicable knowledge for the everyday consumers of intumescent coating systems. The weathering effects on intumescent coating are studied mostly in a laboratory by measuring the solvability of FR coating in water. However, in the real application, the other weathering factors may cause more damage than the moisture. Therefore, this study is more comprehensive. The implementation of MANOVA and ANOVA as statistical methods develops a significant tool in comparing measured data. These methods can determine the repeatability and validity of the conclusions. Despite the popularity of these methods in quality control, the implementation in weathering effects could be almost a new application for the method.

CHAPTER 3: RESERCH METHODOLOGY

3.1 Preparation and Weathering

In this project, three different commercially available intumescent coatings were selected. These three different coatings were labeled A, B, and C. They are described in Table (3). The substrate used in the experiment was AC-grade southern yellow pine 4-ply plywood. The substrates had a nominal thickness of 12.5 *mm*. In the selection process, the specimens from the edges of the wooden panels were discarded in order to avoid bias sampling. As shown in Table (3), the substrates were coated according to the coating instructions by the manufacturers.

Table 3: Coating system overview.

	Description	Coating	Dry Film
Type A	Water-Based, (w/formaldehyde, non-flammable)	1 Layer	0.10 mm
Type B	Latex-Based intumescent coating	1 Layer	0.22 mm
Type C	Water-Based, Water proof, non-combustible	2 Layers	0.37 mm

These three types of coatings were different in description, types A and C were water-based intumescents with type B being latex-based. The type C coating consisted of more layers with thicker dry film [1].

Finally, a total of 363 specimens were selected using a random allocation process. Each specimen had the size of 200*mm* × 100*mm* on average. The specimens were installed on vertical racks at the IBHS Research Center in Richburg, SC, where the

meteorological conditions were monitored by a research-grade surface weathering observing station. The specification of the racks is displayed in Figure 10.

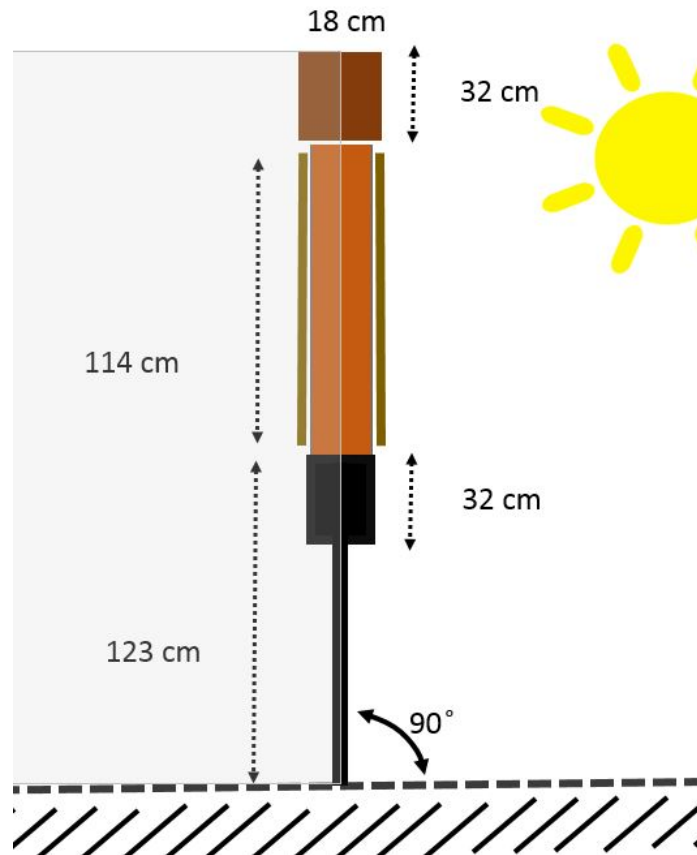


Figure 10: Racks specification

The weathering process had been previously planned for a maximum of 60 months. The starting weathering process dated back to January 2015. However, the project was stopped due to significant loss observed in the coating performance just after 12 months of natural weathering. The details of the weathering timetable is shown in Table (4).

The preparation and weathering process was explained in more detail by Babak Bahrani [1].

Table 4: Timetable of weathering process

	Weathering Interval	Collecting Date
1	0 Months	January 2015
2	3 Months	April 2015
3	6 Months	July 2015
4	12 Months	January 2016

3.2 Measurement Apparatus

In the next step, the combustion properties of the weathered specimens were measured by using a cone calorimeter.

3.2.1 Cone Calorimeter

The schematic cone calorimeter is shown in Figure 11 . This instrument is used to measure the combustibility properties of specimens. The cone heater provides a precise and controllable external heat flux over the sample. The, cone heater consumes electrical power to produce heat, therefore it has no direct part in changing the relative fraction of the chemical gases inside the control volume, shown in Figure 11. This fact guarantees that all changes in the gas composition in the control volume are only from the combustion of the specimen. After the ignition of the specimen the chemical fraction of the gases inside the control volume change. These gases are sucked into the gas analyzer from the exhaust duct, and the combustion details are revealed through the measuring of oxygen, carbon monoxide, and dioxide mole fractions. In the entire process of the combustion, the weight of the specimens is precisely recorded for thermogravimetric analyses. The mass deterioration is an important factor to predict the resistance of structures in the WUI fires.

3.2.2 Oxygen Consumption Calorimetry Principles

The main idea of the Oxygen Consumption Calorimetry dates back to 1917. During the Great War, Thornton published interesting results of measuring heat released per unit mass of oxygen consumed in complete combustion. The report included the results of combustions for a large number of organic liquids. Thornton showed that in a complete combustion of almost every organic liquid, the net heat released is almost constant per unit mass of consumed oxygen [102]. In 1980, Huggett reported the same conclusion, but this time for organic solid fuels. Huggett also measured the constant value of heat released per unit mass of consumed oxygen [103]. In average, the energy released for each kilogram of oxygen consumption is 13.1 MJ. There are few exceptions, however the calculation is almost 95% accurate.

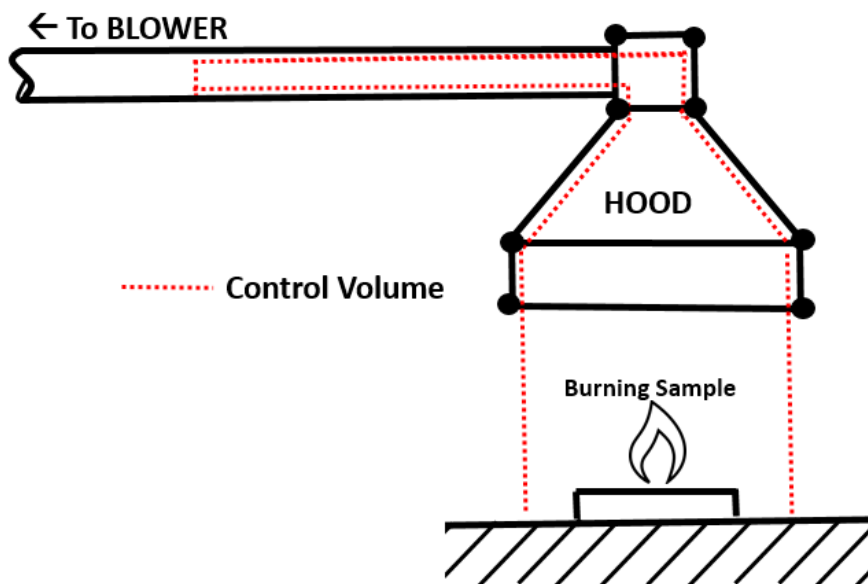


Figure 11: Cone Calorimetry and control volume used in calculation of oxygen consumption

Since discovery, engineers have designed several types of designs used for Oxygen Consumption Calorimetry. In most of the designs, just like shown in Figure 11, a control volume surrounds the combustive fuel. The oxygen consumption is calculated by comparing the mole fraction of oxygen in the exhaust duct with the normal fraction of the oxygen in the laboratory air [104].

The heat release rate as a function of time, $\dot{Q}(t)$, is calculated using the measured values and the equation (5) below.

$$\dot{Q}(t) = \left(\frac{\Delta h_c}{r_o} \right) (1.10) C \sqrt{\frac{\Delta P}{T_e}} \frac{(x_{O_2}(0) - x_{O_2}(t))}{1.105 - 1.5 x_{O_2}(t)} \quad (5)$$

T_e : Absolute temperature of gas [k]

$x_{O_2}(t)$: Oxygen analyzer reading

ΔP : Pressure differential [Pa]

C : C-factor is the coefficient which used to calibrate the cone calorimeter. This factor is known for well-defined methane burning test.

In equation (5), the constant coefficient, $\left(\frac{\Delta h_c}{r_o}\right)$, has the value of $(13.1 \times 10^3 kJ/kg O_2)$.

The other quantities in the equation are measured by instruments installed on the Cone Calorimeter. These quantities are as follows:

3.2.3 Combustion Property in Calorimetry

In calorimetry, the Heat Release Rate (HRR) as a function of time is one of the most important quantities used in fire protection analysis. HRR can affect the rate of fire growth. The HRR as function of time can show the maximum HRR and the time

when the maximum release of energy happens due to combustion. In this project, the average of HRR was used for statistical analysis. The lower average in HRR displays that the heat energy released in a relatively long time in a lower amount. Time to Ignition (TTI) is also shown in HRR graph , however, it is more precise to use a stopwatch to measure TTI.

The other important quantity is the Mass Loss Rate (MLR). MLR can show the sustainability of the structure against fire. MLR is calculated from the slope of the curve of specimen mass vs. time. In most of the cases, the average of MLR from 10% loss of the initial mass to 90% loss of the initial mass, $\dot{m}_{A,10-90}$, is used to determine the fire resistance of the material. The higher average of MLR shows a faster mass loss in combustion. Also, it shows potentially higher HRR and faster fire growth.

The behavior of Effective Heat of Combustion (EHC) plays a crucial role in the magnitude of fire damage. EHC is defined as the effective heat released per unit of mass loss. The EHC is proportional to heat release rate divided by mass loss rate, however the EHC is reported automatically by cone calorimeter software. It would be disastrous that combustion happens in the materials with the ability to produce a high amount of heat per unit mass. This quantity shows how much energy is produced by consuming the unit mass of the fuel. For good fuel, the average value of EHC is high, however, in fire protection, it is not a good idea to build structures with materials which have a high EHC. The coating which applied to protect the substrate should not increase the EHC. The weathering contribution to the EHC of

intumescent coatings was studied in this project. Increasing EHC due to weathering is defined as adding fuel to the structure which essentially causes a large fire with a higher potential of damage.

Cone Calorimeters measure several other combustion properties [1]. However, these four quantities (TTI, HRR, MLR, and EHC) were used for this project.

3.3 Critical Heat Flux

Critical heat flux is an important combustion property which can be used to explain the weathering effects on the intumescent coatings. There are two main reasons explaining the importance of measuring critical heat flux (q''_{cr}) in the investigation of the weathering effects on fire retardant materials. First, with the fact that materials having a higher critical heat flux to ignition, suggests that the materials serve as a better fire resistance substance. Second, the critical heat flux is a response quantity which is not explicitly a function of effective heat flux (q''_e). In the lack of appropriate information of the range of effective heat fluxes in possible fires, the critical heat flux can provide applicable information to compare the effectiveness of fire retardant materials. In many cases, the risk and range of the effective heat flux are unknown, therefore the critical heat flux could be really useful. It is important to recall many combustion properties such as TTI, HRR, and MLR, in general, are explicit functions of effective heat flux.

Two simplified models can be used to calculate the critical heat flux; thermally thick solid and thermally thin solid models [105].

In thermally thick solid model shown in Figure 12, It was assumed that the sample

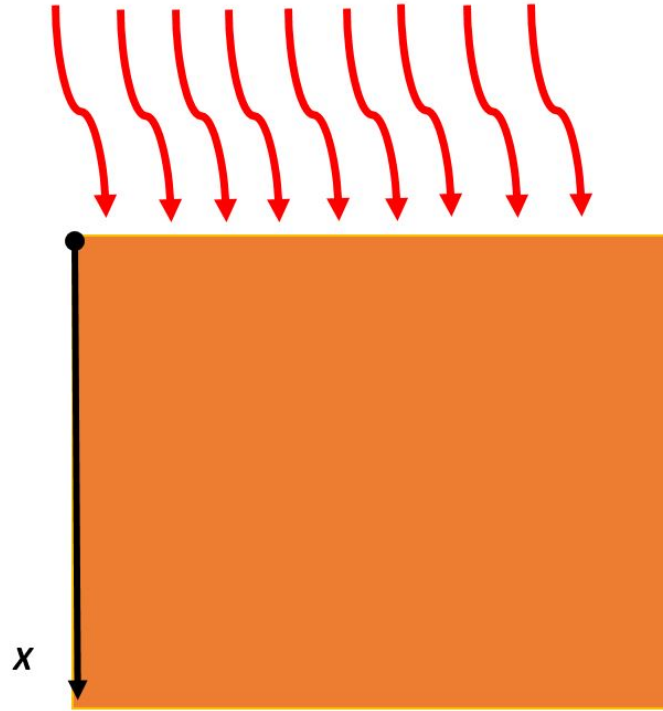


Figure 12: Thermally thick solid sample under constant heat flux

is thick enough that the heat flux from front face never reaches the back face of the sample before the ignition. The thermally thick model is presented in following formulation [106];

$$\dot{q}_e'' = q_{cr}'' \left[1 + 0.73 \left(\frac{k\rho c}{h_{ig}^2 t_{ig}} \right)^{0.547} \right] \quad (6)$$

The equation (6) is used to calculate the critical heat flux (q_{cr}''). As shown in Figure 13, the intersection of the effective heat flux (\dot{q}_e'') axis and the best fitted line of transformed ignition time, $t_{ig}^{-0.55}$, determines the critical heat flux for the samples [105].

In the thermally thin solid model shown in Figure 14 , the temperature of the sample is assumed uniformly change by time. In this model, the back face of the

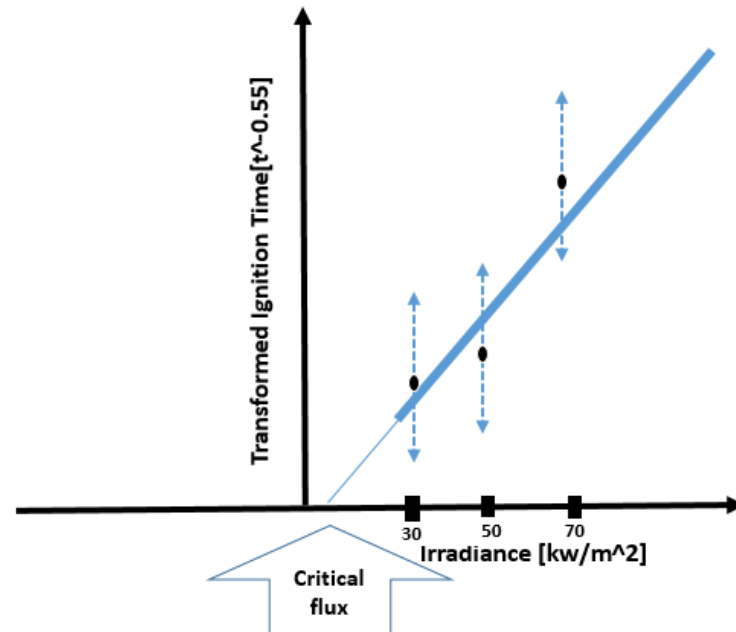


Figure 13: Method of measuring critical heat flux

sample is perfectly insulated (shown in Figure 14). In practice, the ceramic isolator is used beneath the sample. Janssens numerically solved the equation of thermally thin solid system [107]. It was found that in the case of thermally thin solid, the plot of the inverse of time to ignition (t_{ig}^{-1}) as a function of effective heat flux (\dot{q}_e'') can be presented as a straight line. The intersection of the line with the heat flux axis is the critical heat flux for the thermally thin samples [105].

In fire protection, materials with higher critical heat flux are more preferred due to their better resistance against heat in fires. It is important to remember that these two models are simplified to explain burning a simple fuel in one phase. In the case of the coated sample, several phase transitions occur before the actual combustions. These phases are parts of the intumescent mechanism. Therefore, these models may only provide approximate results. In addition, the minimum heat flux of 30 kW/m^2

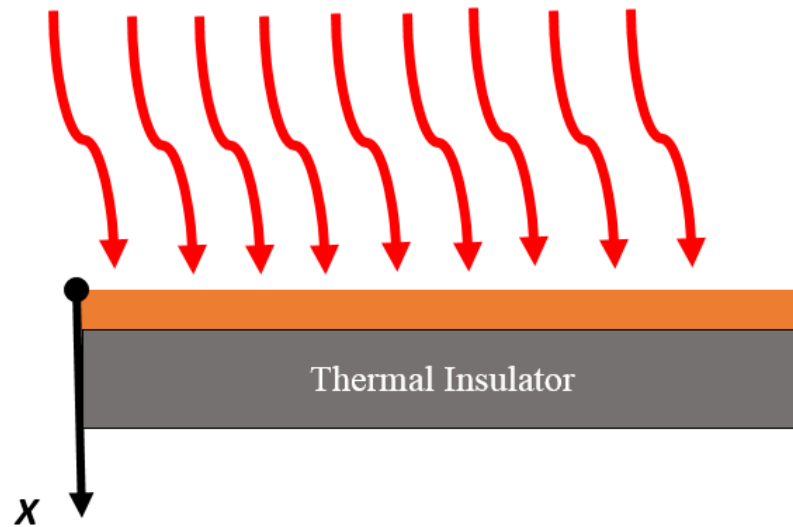


Figure 14: Thermally thin solid sample under constant heat flux

for testing samples with the nominal thickness of 12.5 mm are more similar to the condition of thermally thin solid model assumptions. Therefore, it was predicted that this model would provide better results.

3.4 Road Map of Project

In this project, the weathering effects on the fire retardant intumescent coatings was investigated. Three different types of coatings were selected. The baseline data was collected from measuring combustion properties of uncoated specimens. After three months, the first weathered specimens were collected from the rack and tested by cone calorimeter. The same procedures were repeated after six and twelve months. The data were analyzed using the ANOVA and MANOVA methods.

The project objective was to compare the performance of weathered coated spec-

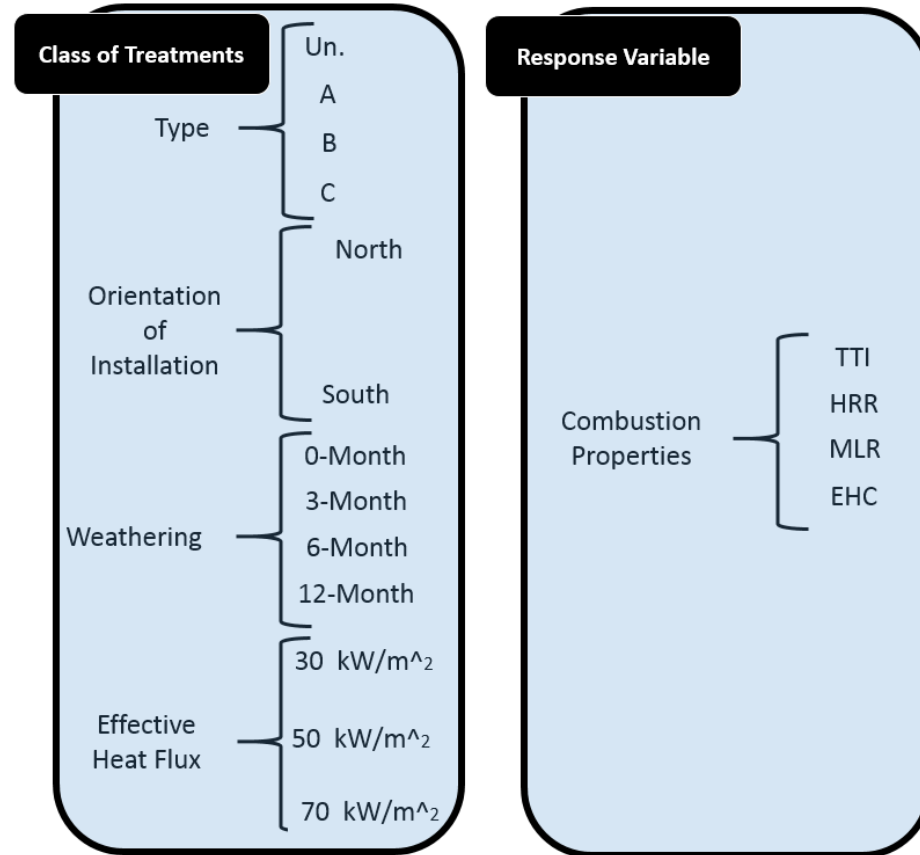


Figure 15: Degree of freedoms in the weathering effect study

imens with the baseline formed by the uncoated specimens. The statistical evidence can scientifically show whether the coating was useful or useless after weathering. Also, these methods could determine how long the coating protection last.

To achieve the objective, the performance of intumescent coatings under weathering was examined. As shown in Figure 15, the data consisted of combustion properties of three different coating types (labeled A, B, and C) plus uncoated specimens. In the weathering process, four different weathering interval (0, 3, 6 and 12 months) plus the two different orientations of installation (southward and northward) were considered. Also, in cone calorimetry, three different effective heat fluxes (30, 50 and 70 kW/m^2) were used. The total degree of freedom (different treatments of the specimens) was

96. In each of these 96 classes, three specimens were used to measure the combustion properties. TTI, HRR, MLR, and EHC values populated the raw data of the statistical analysis. The total sample size around 384 number was used to investigate the weathering effects on the performance of intumescent coatings.

The first step was to determine the importance of each class of treatments. The reduction of the degree of freedom could simplify the understanding of weathering effects on the coating performance. Multivariate analysis of variance (MANOVA) is a suitable method to rank the importance of the classes. In a case that a treatment was not effective in measured data, the elimination of corresponding class would be reasonable. Another useful approach to investigate the rank of importance is by using machine learning methods such as decision tree for multi-class classification. This process was done according to the flowchart shown in Figure 16.

In the second step, the weathering effects on each type was investigated by using analysis of variance (ANOVA). In this stage, the data would present the behavior of each class in different weathering time. In a case that ANOVA would display that the weathering was effective, the plotted bar chart showed the trend of the response variable in different weathering time intervals. This process was done according to the flowchart shown in Figure 17.

In the third step, the advantage of the coatings was investigated. In this part of the analysis, the uncoated counterparts were used as the reference to determine the performance of each type of coating. Based on the flowchart shown in Figure 18, the effective interval for each type of coating was determined.

The last part of the results analysis was dedicated to the results of critical heat

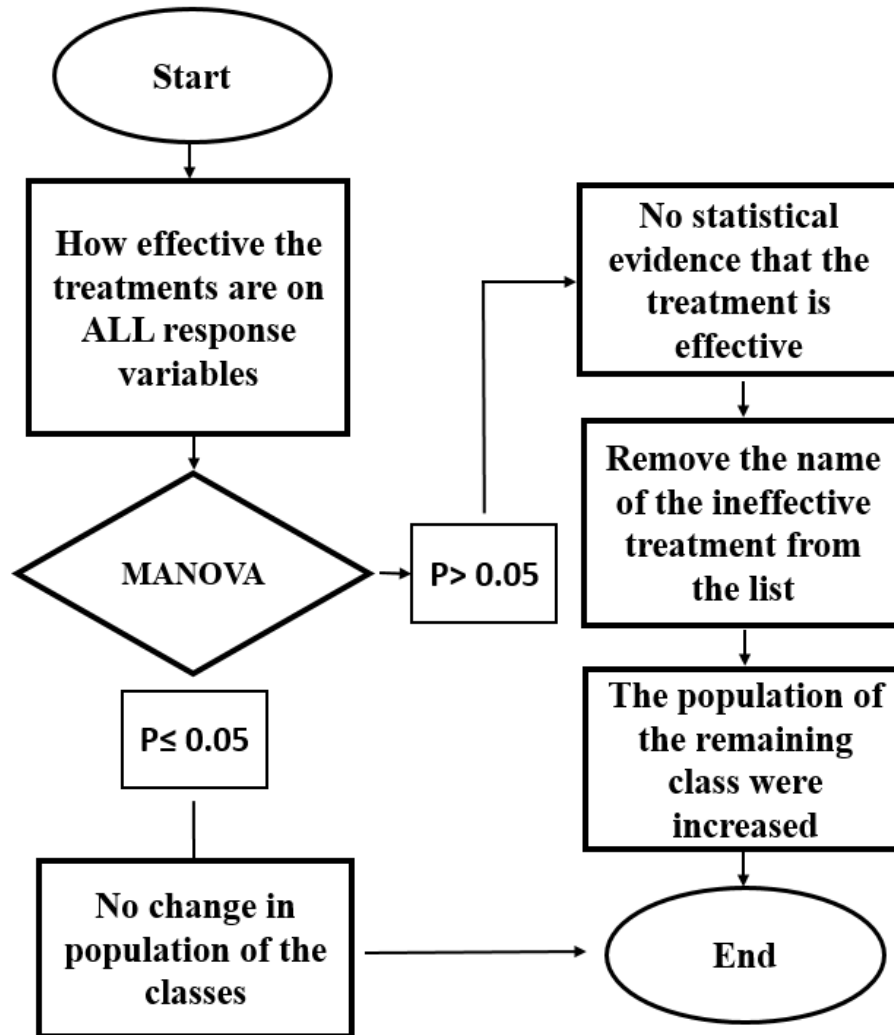


Figure 16: Flowchart to find effective treatments

flux. The critical heat flux can be used to investigate the performance of the coatings under weathering effects. The higher critical heat flux in materials suggests that the materials serve as a better fire resistance substances. Second, the critical heat flux is a response quantity which is not explicitly a function of effective heat flux. In most of the fires, the level of effective heat flux is not known. The critical heat flux in this regard is more comprehensive due to its independence from effective heat flux.

In the fifth chapter, the summary, conclusion, and recommendation for future research

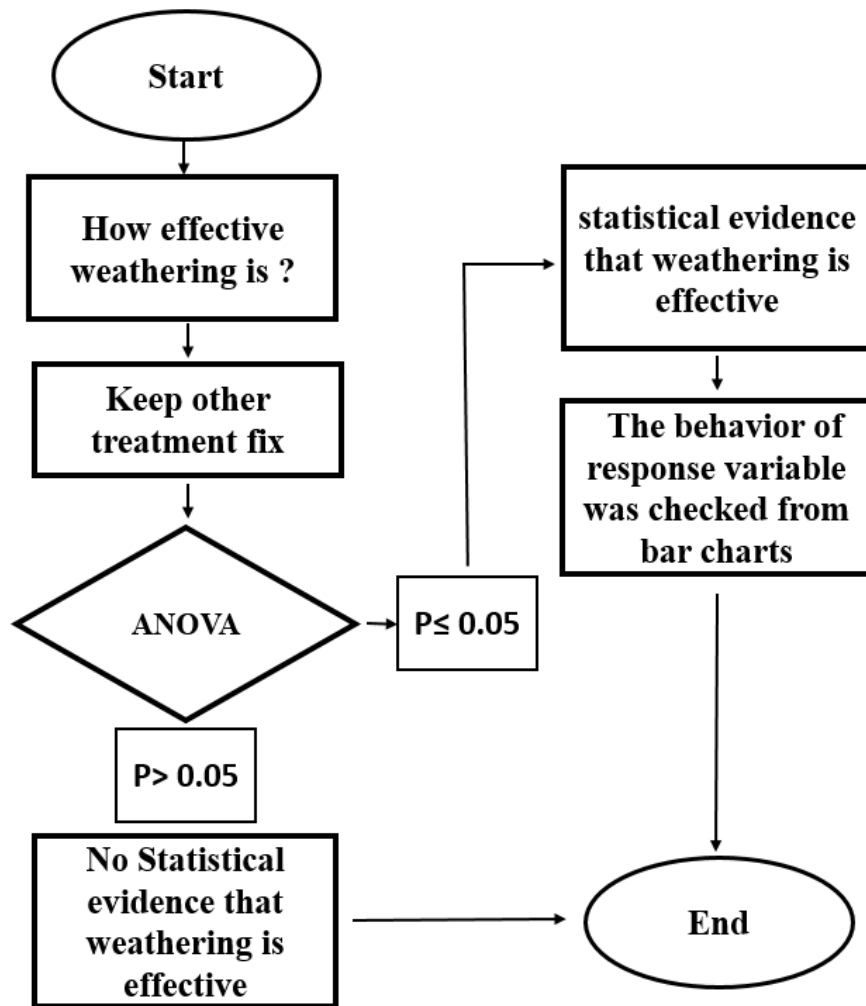


Figure 17: Flowchart to investigate weathering effects

would be presented.

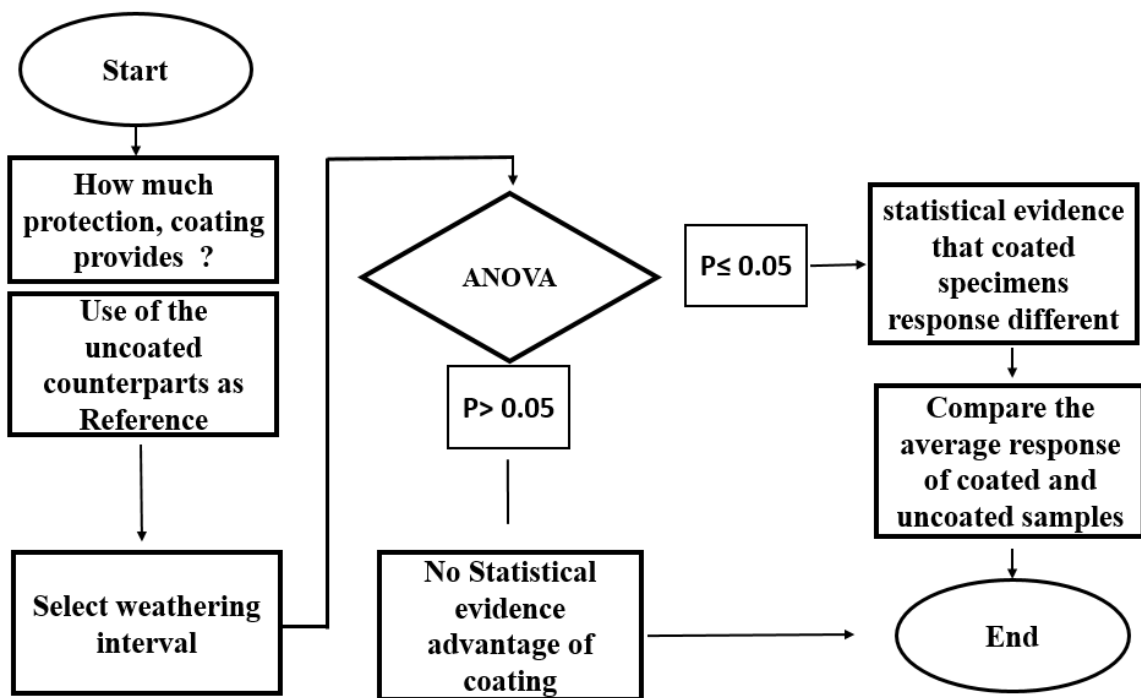


Figure 18: Flowchart to investigate coating effects

CHAPTER 4: DATA ANALYSIS

On the first step, MANOVA was employed to investigate the effects of all causes on the performance of the intumescent coatings. The causes in our case include; weathering duration (0,3,6 and 12 months), orientation of installation (southward and northward), effective heat fluxes (low, medium and high flux) and type of coating (A, B, C and uncoated). In this part, all data which includes weathering duration, orientation, effective heat flux and coating were used to determine whether these treatments are effective or not.

The raw data used in this chapter are listed in the Appendix A. In the MANOVA, the entire data was used.

Table 5: MANOVA results for all different treatments.

Causes/Treatments	TTI	HRR	EHC	MLR
Weathering (W)	0.0000	0.0000	0.0000	0.0000
Orientation (O)	0.0602	0.9354	0.2598	0.8028
Heat Flux (H)	0.0000	0.0000	0.0291	0.0000
Type of Coating (T)	0.0000	0.0000	0.0000	0.0000
W interaction with O	0.2125	0.9263	0.2279	0.9203
W interaction with H	0.0000	0.0000	0.0000	0.0000
W interaction with T	0.0534	0.0000	0.0345	0.0000
O interaction with H	0.0984	0.6676	0.5558	0.3455
O interaction with T	0.0702	0.2392	0.7503	0.0512
H interaction with T	0.0000	0.0000	0.0001	0.0009

Table (5) shows the P-value results from the MANOVA test.

The calculated P-values (which are less than 0.05), shown in bold font, reject the null hypothesis for the effect of weathering, heat flux and type of coatings. Furthermore, these three factors in interaction are clearly effective on response variables. The only exception was seen in the effect of interaction between weathering and type of coating on the TTI ($P - value = 0.0534$). The orientation of installation did not show precipitable effectiveness. All P-values calculated for orientation and its interaction with the other factors confirmed null hypothesis (greater than 0.05). There was no statistical avoidance to accept that changing the orientation of installation caused a clear change in combustion properties of the samples. Therefore, it could be reasonable to eliminate the factor of orientation of installation from the list of causes in the rest of this study.

Another approach to rank the treatments from the most to least effective is the machine learning approach.

A machine learning method to estimate the importance of the involved parameters in the combustion properties was employed. Based on the type of the involved parameters, the binary classification decision tree for multiclass classification was selected. To check the importance of each predictor (Weathering, coating, heat flux and orientation of installation) to predict the response (TTI and HRR), first, we used fit-tree function available in MATLAB. The binary classification decision tree based on the inputted response is returned by this function. In this stage, the entire data set was used as training regression set. Second, another function in MATLAB which returns the estimate predictor importance values was employed. The estimate predictor importance value (the value of Y axis in the plotted bar chart Figure 19 and Figure 20)

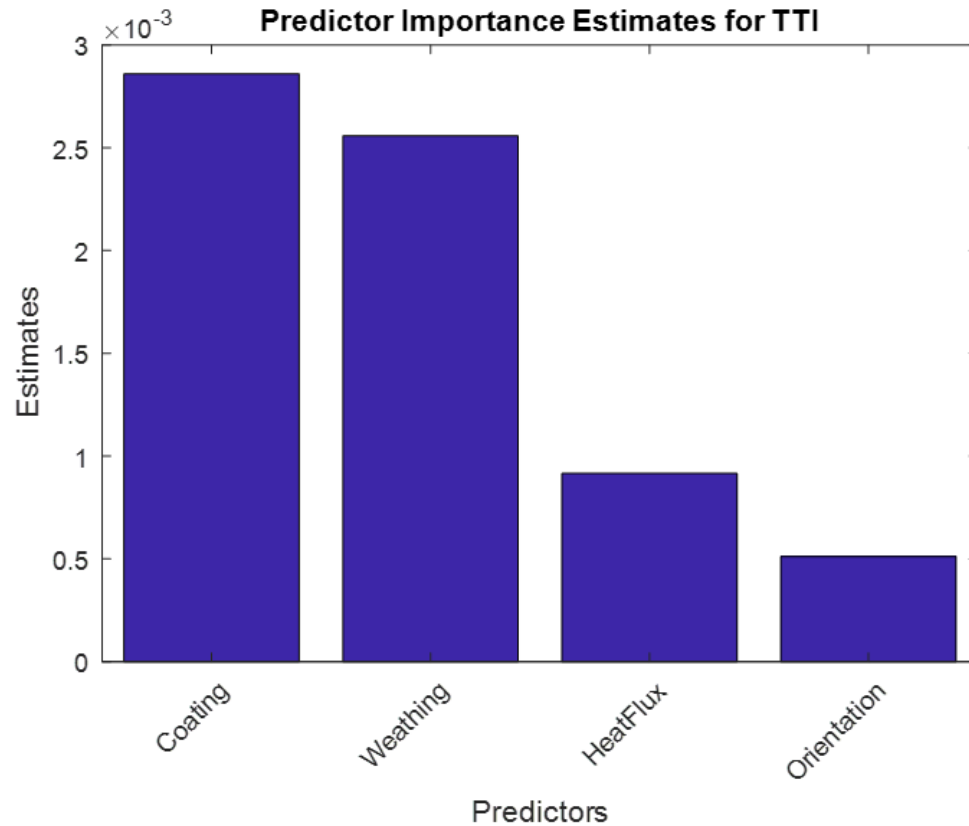


Figure 19: Predictor Importance for TTI

is defined as entire changes (summing all changes) in the risk because of splitting on every predictor divided by the number of branch nodes in the fitted tree model. The high value for a predictor shows the importance of the predictor in the response. The minimum possible value is zero showing no role of the corresponding predictor in the response of the system.

As shown in Figure 19, coating played the most important role in determining TTI of the all samples with the different coating, weathering, effective heat flux and orientation of installation (Northward and Southward). As the second rank, weathering duration, was also an important factor which justifies the importance of this project.

In consistency with MANOVA results, the orientation of installation showed the least

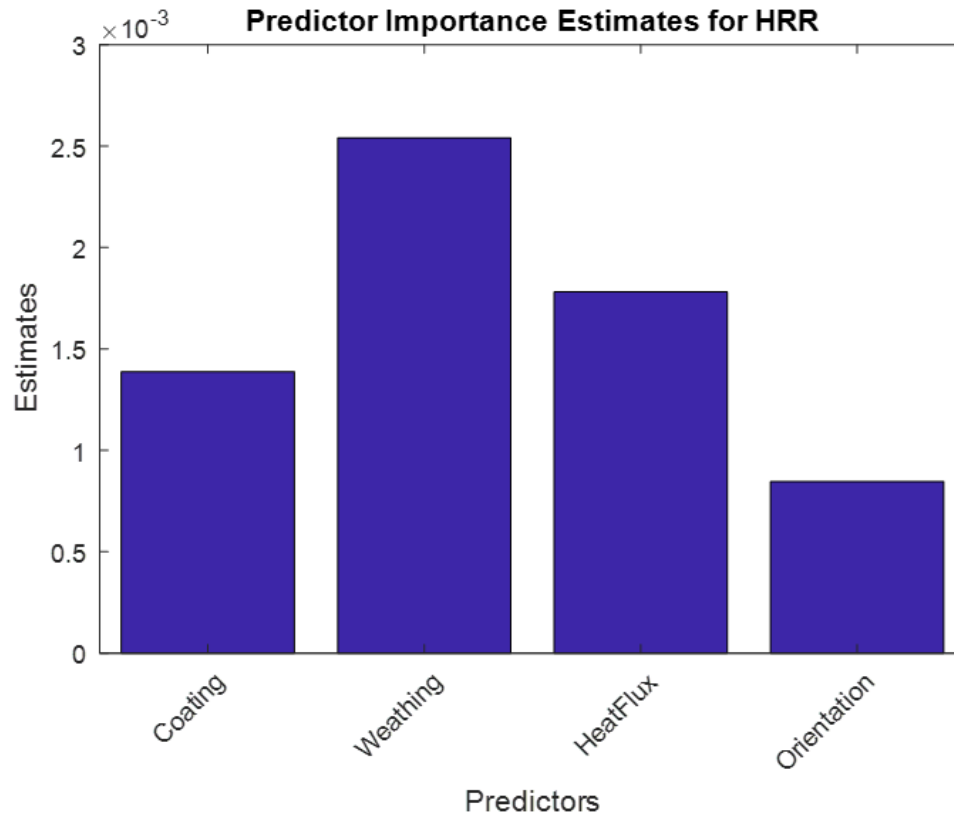


Figure 20: Predictor Importance for HRR

importance in determining TTI.

As shown in Figure 20, weathering duration, and heat flux played the most important role in determining HRR of the all samples with the different coating, weathering, effective heat flux and orientation of installation (Northward and Southward). The rank of coating in TTI was replaced by effective heat flux for prediction of HRR (see Figure 19). In addition, weathering showed almost the same importance in both TTI and HRR. In consistency with MANOVA results, the orientation of installation showed the least importance in determining HRR. It is notable that HRR is an important factor in fire spread phase. It was observed that the natural weathering and effective heat flux was more important than type of intumescent in fire propagation phase.

4.1 Low Heat Flux Test

The combustion properties of the specimens in the low heat flux ($30 \text{ kW}/\text{m}^2$) tests are presented in this chapter. Studies showed that relatively long exposure time to the low heat flux occurred in real fires [101]. Therefore, the results of the low heat flux tests can be critical to estimate the performance of coating in real fires.

The TTI, average HRR, average MLR from 10% loss to 90% loss and EHC results from cone calorimetry tests were appointed for ANOVA tests.

4.1.1 TTI in Low Heat Flux Test

TTI is one of the most important factors in fire retardant performance. Longer TTI could benefit fire management in both ignition phase and propagation phase.

Figure 21 shows the effect of weathering on TTI of specimens which coated with three different FR coatings. The four dashed lines in the graph show the base lines (the mean value of TTI in uncoated specimens) in different weathering duration. The P-values, calculated by ANOVA for each type of coating, are listed below the graph. For Types A and B, the null hypothesis is rejected according to calculated P-values (P-values less than 0.05). Statistically, the clear shifts in the measured TTI were observed. These shifts showed decreasing by increasing weathering time. In type C, the null hypothesis is still valid (P-value greater than 0.05). Meaning there is no statistical evidence that weathering duration affected the performance of the coating even after 12 months. Demonstrating the advantage of using type C rather than types A and B.

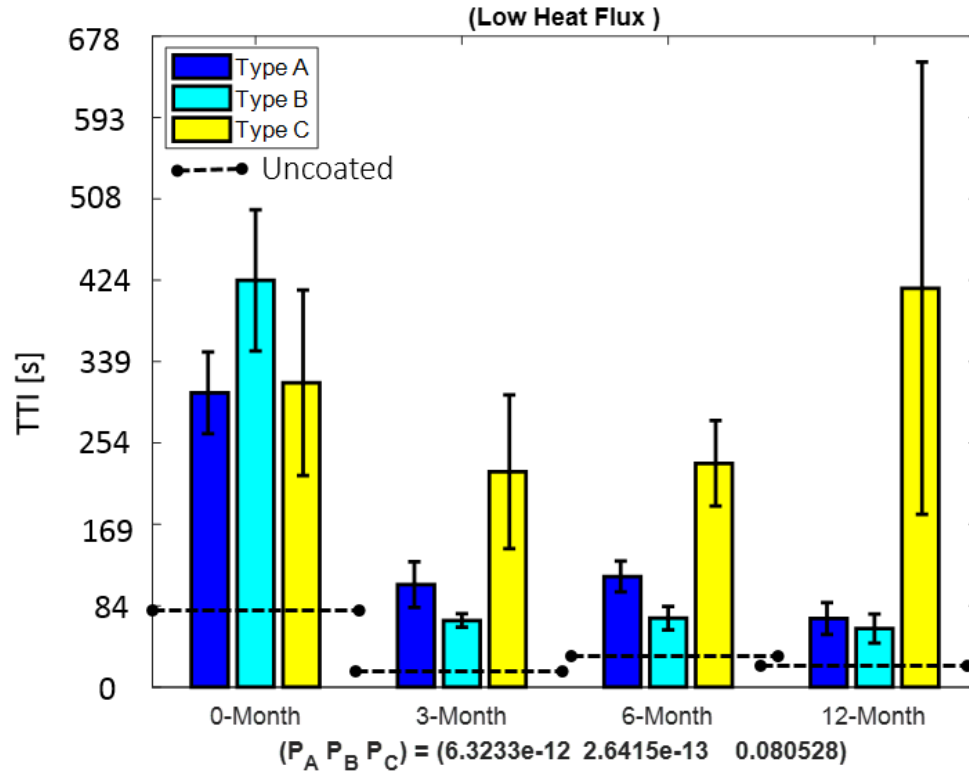


Figure 21: Effect of weathering on TTI in low heat flux test

Next, the advantages of the coatings was investigated by comparing TTI of coated and uncoated specimens in low heat flux tests. The P-values are listed in the Table (6). In all cases, the performance of coated specimens is different from the performance of the uncoated counterparts, except two cases which are shown in bold font in Table (6). The weathering damage on the performance of the type B coating just after 6 months was severe. There was no statistical evidence that type B had any advantage after 6 months than uncoated samples. It seems that renewing the coating type B must be considered just before 6 months. In the case of type A, despite clear weathering degradation, The coating was working and its performance clearly was better than uncoated counterparts even after 12 months of weathering.

In next step, the average of TTI of coated specimens was subtracted with the

Table 6: P-values comparing performance of coated from uncoated counterparts in TTI under low heat flux.

	0-Month	3-Month	6-Month	12-Month
Type A	0.0000	0.0000	0.0003	0.0163
Type B	0.0000	0.0000	0.1626	0.0887
Type C	0.0001	0.0002	0.0000	0.0032

Table 7: Change in average of TTI in second because of coating in low heat flux tests.

	0-Month	3-Month	6-Month	12-Month
Type A	227	73	58	28
Type B	345	36	14	17
Type C	238	191	176	372

average TTI of uncoated counterparts. The results are listed in Table (7). The positive values in the table show that in all the cases the TTI of coated specimens is longer than uncoated counterparts. Based on ANOVA results (shown in Table (6)), all of the reported numbers in Table (7) can be assumed repeatable, except the numbers in bold font (B type in 6 and 12 Months).

It is clear from the Figure 21 that uncoated samples were also affected by weathering and TTI decreased especially in the first 3 months.

The results of TTI in low heat flux tests showed that the Type C is not affected by weathering and this type preserved its performance. In type A, the weathering effects were clear, however, this type showed a better performance than the uncoated even after 12 months of weathering, despite clear weathering degradation. In the case of type B, weathering degradation causes serious damage in performance. Any advantage of the coating was not seen after 6 months and 12 months in weathered samples of type B.

4.1.2 HRR in Low Heat Flux Test

The HRR is an important factor in propagation phase of a fire. The lower HRR can slow down the fire propagation. Each structure in a fire can be a source of ignition to the adjacent potential fuel. The ignition of the surrounding fuel is less probable if the structure burns with lower HRR. Moreover, slower fire propagations give more time for mobilizing the firefighting efforts.

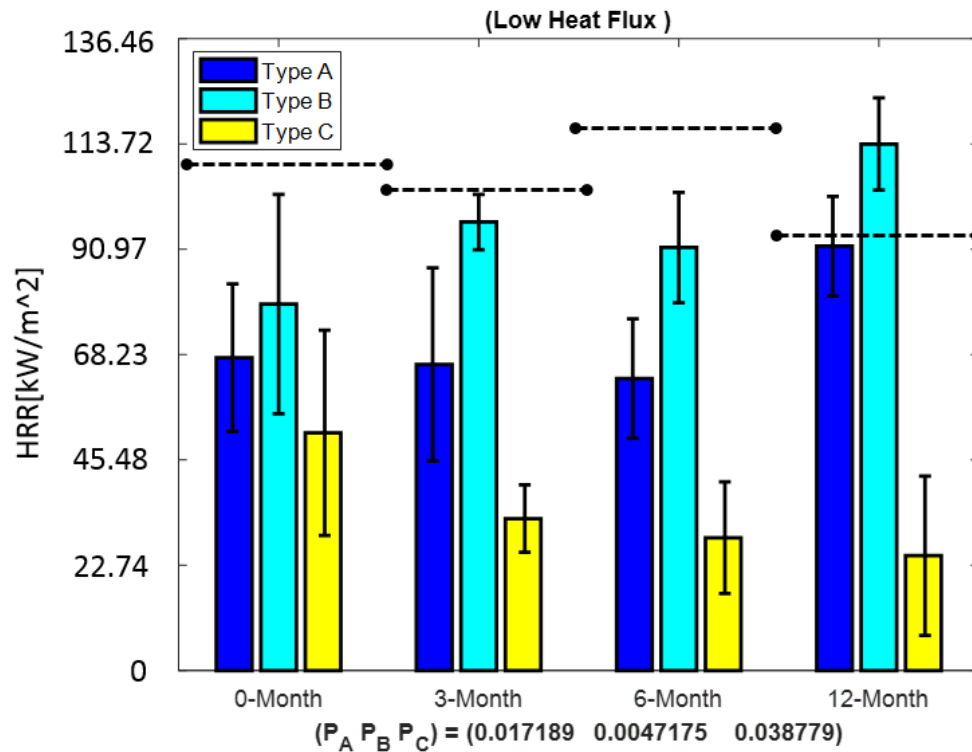


Figure 22: Effect of weathering on HRR in low heat flux test

Figure 22 shows that the weathering effects on the HRR in low heat flux tests. The four dashed lines in the graph show the base lines (the mean value of HRR in uncoated specimens) in different weathering duration. In addition, the P-values of the effect of weathering on each type are listed beneath the graph.

The reported P-values confirm the weathering effects on HRR for all types. The null hypothesis is rejected, and it is shown in the relatively small P-values (less than 0.05). However, there is a significant difference in behavior of type C, shown in Figure 22. The performance of type C was improving with increased weathering time. This improvement was confirmed by ANOVA results (P-value less than 0.05). On the other hand, the performance of type A and B was reduced with increased weathering time.

Table 8: P-values comparing performance of coated from uncoated counterparts in HRR under low heat flux.

	0-Month	3-Month	6-Month	12-Month
Type A	0.0001	0.0014	0.0001	0.5371
Type B	0.0133	0.0272	0.0064	<u>0.0057</u>
Type C	0.0001	0.0000	0.0000	0.0000

Table 9: Change in average of HRR in kW/m^2 because of coating in low heat flux tests.

	0-Month	3-Month	6-Month	12-Month
Type A	-41.47	-37.38	-59.43	-3.54
Type B	-29.90	-6.62	-31.13	<u>18.51</u>
Type C	-57.68	-70.67	-93.18	-70.41

The results of analysis between the HRR of the coated specimens and uncoated counterparts are listed in Table (8). All the reported P-values reject null hypothesis, which means that the coated and uncoated specimens had different responses, except type A in 12 months of weathering. Meaning that the advantage of using type A disappeared in this case (12 months weathering).

In Table (9), the average shift in HRR of coated specimens from uncoated coun-

terparts is listed. As seen in Table (9), the calculated values are negative for all cases except one case (type B/12-Month). This means that coating decreased the HRR which is good from the fire protection point of view. Although, the repeatability of these shifts was almost certain (P-values less than 0.05) except for type A/12-Months (see Table (8)). The interesting result is the positive value for type B/12-Months. This means that the performance of B coating in 12 months of weathering was even poorer than uncoated counterparts, and surprisingly, this inferiority had high portability to be repeated (see Table (8)).

In the low heat flux tests, type C showed remarkable performance which improved with increased weathering time. In type A, the performance decreased by weathering. In the 12-month data, there was no sign of protection from the A type coating. Type B demonstrated the poorest performance. The performance of type B was even poorer than uncoated counterpart in 12 months of weathering.

4.1.3 MLR in Low Heat Flux Test

MLR is an important factor, which can display the rate of destruction of the samples under heat flux. Figure 23 shows the effects of weathering on MLR of the coated specimens in low heat flux tests. The four dashed lines on the graph display the base lines (the mean value of MLR in uncoated specimens) in the different weathering durations.

In addition, the P-values for each coating type is reported under the graph in Figure 23. These values are the ANOVA results when the weathering effects were

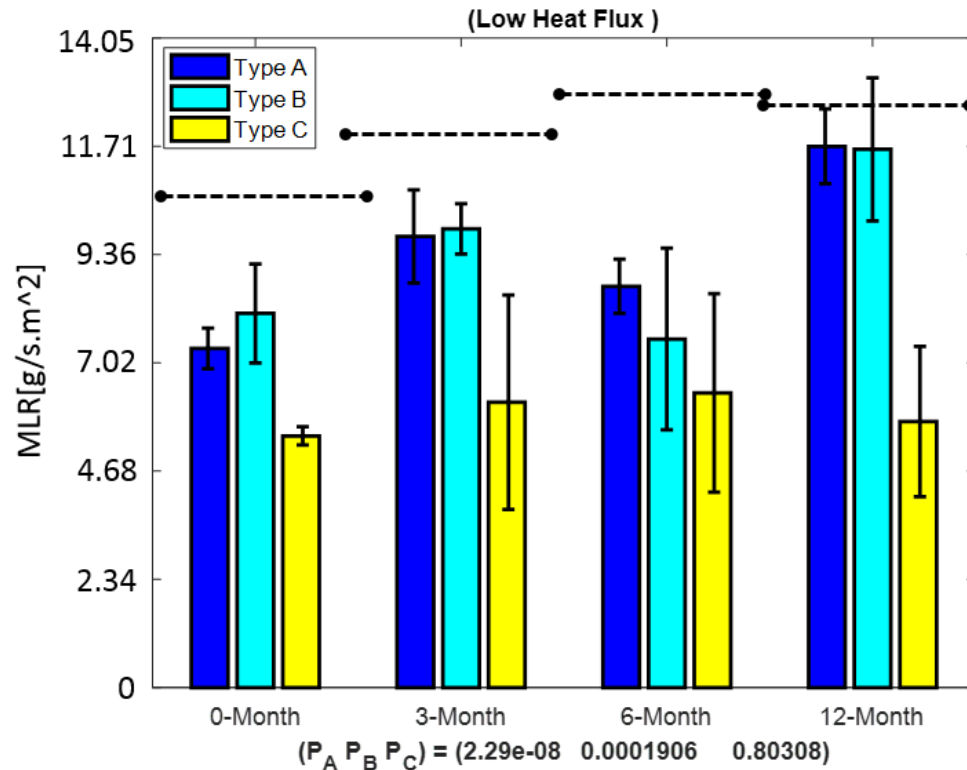


Figure 23: Effect of weathering on MLR in low heat flux test

investigated. It is important to remember that lower MLR shows better protection in a fire. The calculated P-values for type A and B rejected the null hypothesis. It means that weathering caused a clear change in measured MLR of the samples. The bar chart (Figure 23) shows that the MLR increased by weathering. In the case of type C, the ANOVA result (P-value greater than 0.05) confirmed the null hypothesis. It means that there was no statistical evidence that weathering affect the performance of the samples. This conclusion is also confirmed by bar chart in Figure 23.

The calculated P-values in comparing MLR of coated specimens with uncoated counterparts are shown in Table (10). In all cases, the P-values rejected the null hypothesis, except type A and B in 12 months weathering. This shows that the

Table 10: P-values comparing performance of coated from uncoated counterparts in MLR under low heat flux.

	0-Month	3-Month	6-Month	12-Month
Type A	0.0004	0.0323	0.0001	0.0536
Type B	0.0066	0.0320	0.0003	0.1978
Type C	0.0000	0.0008	0.0001	0.0000

Table 11: Change in average of MLR in $gr/s.m^2$ because of coating in low heat flux tests.

	0-Month	3-Month	6-Month	12-Month
Type A	-3.33	-2.22	-4.24	-0.85
Type B	-2.57	-2.05	-5.38	-0.91
Type C	-5.22	-5.81	-6.54	-6.80

performance of the coated specimens was different from uncoated. However, this advantage disappeared just in 12 months weathering in type A and B. For type C, the advantage of coating was seen even after 12 months of weathering.

In Table (11), the average MLR shifts in coated specimens from uncoated counterparts are listed. As can be seen from the table, all the values are negative, which means the performance of the coated specimens was better in MLR. However, the performance of type A and B in 12 months weathering was not considered repeatable based on P-values reported in Table (10).

Type C showed the best performance. The type C coated specimens were not affected seriously by weathering even after 12 months. In addition, the MLR of type C coated specimens were clearly smaller than uncoated counterparts. The type A and B coated specimens were affected by weathering, and in the results of MLR in 12 months weathering, the advantage of coating was not seen.

4.1.4 EHC in Low Heat Flux Test

The averages of EHC results for coated samples are plotted in Figure 24. The four dashed lines in the graph show the base lines (the mean value of EHC in uncoated specimens) in the different weathering durations. The P-values of the weathering effects on EHC for each type are listed below the graph. The P-values demonstrated that weathering affected the EHC. The interesting behavior of decreasing of EHC by weathering was seen in all the types of coatings. It means the performance of coating improved by weathering.

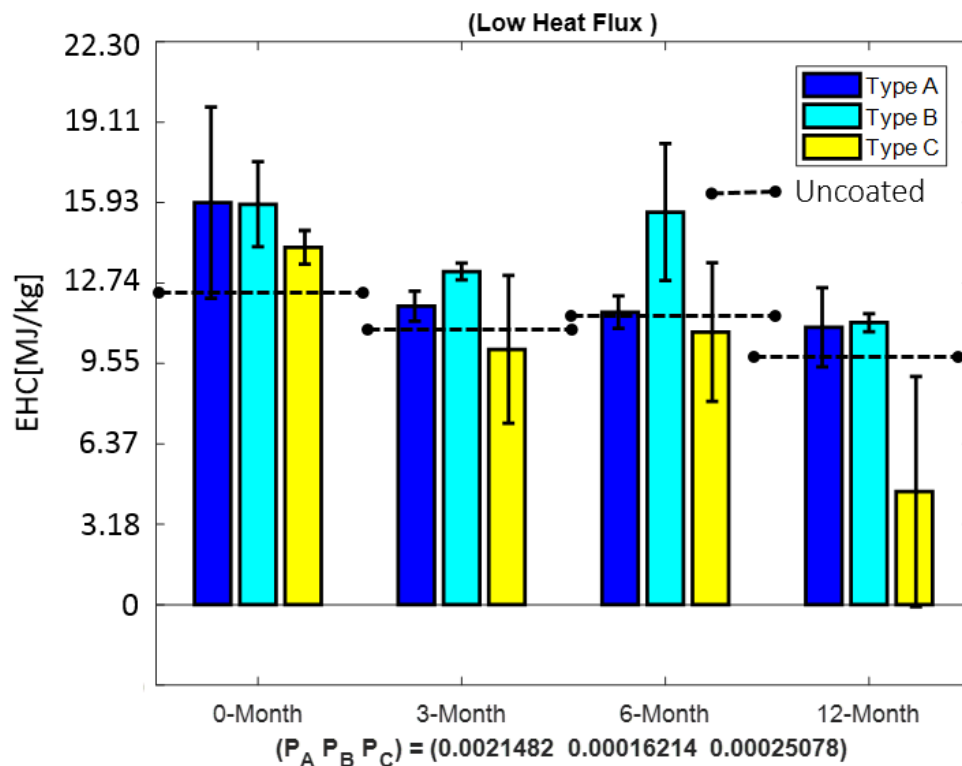


Figure 24: Effect of weathering on EHC in low heat flux test

In the next step, the shift in average EHC of specimens from the uncoated counterparts was calculated. The results are listed in Table (12). The positive values

depict that the EHC of coated specimen was greater than uncoated counterparts. The negative values were only seen in type C. It is important to recall that material with less EHC produces less heat in combustion. It seems that there was a natural process that decreasing EHC of the specimens by passing time.

The P-values of comparing coated with uncoated counterparts are listed in Table (13). In four cases shown by bold font, the null hypothesis was confirmed.

Table 12: Change in average of EHC in MJ/kg because of coating in low heat flux tests.

	0-Month	3-Month	6-Month	12-Month
Type A	3.64	1.02	0.39	1.10
Type B	3.58	2.39	4.35	1.28
Type C	1.87	-0.69	-0.39	-5.40

Table 13: P-values comparing performance of coated from uncoated counterparts in EHC under low heat flux.

	0-Month	3-Month	6-Month	12-Month
Type A	0.0476	0.0356	0.1722	0.1192
Type B	0.0015	0.0001	0.0028	0.0000
Type C	0.0060	0.5902	0.7345	0.0158

4.2 Medium Heat Flux Test

The results of the medium heat flux ($50 \text{ kW}/\text{m}^2$) tests are presented in this section. The exposure duration of medium heat flux is much shorter than the exposure duration of low heat flux in a real fire [101]. However, the damage caused by higher heat flux could be more serious.

4.2.1 TTI in Medium Heat Flux Test

TTI is one of the most important factors in fire retardant performance. Longer TTI could benefit fire management in both ignition phase and propagation phase.

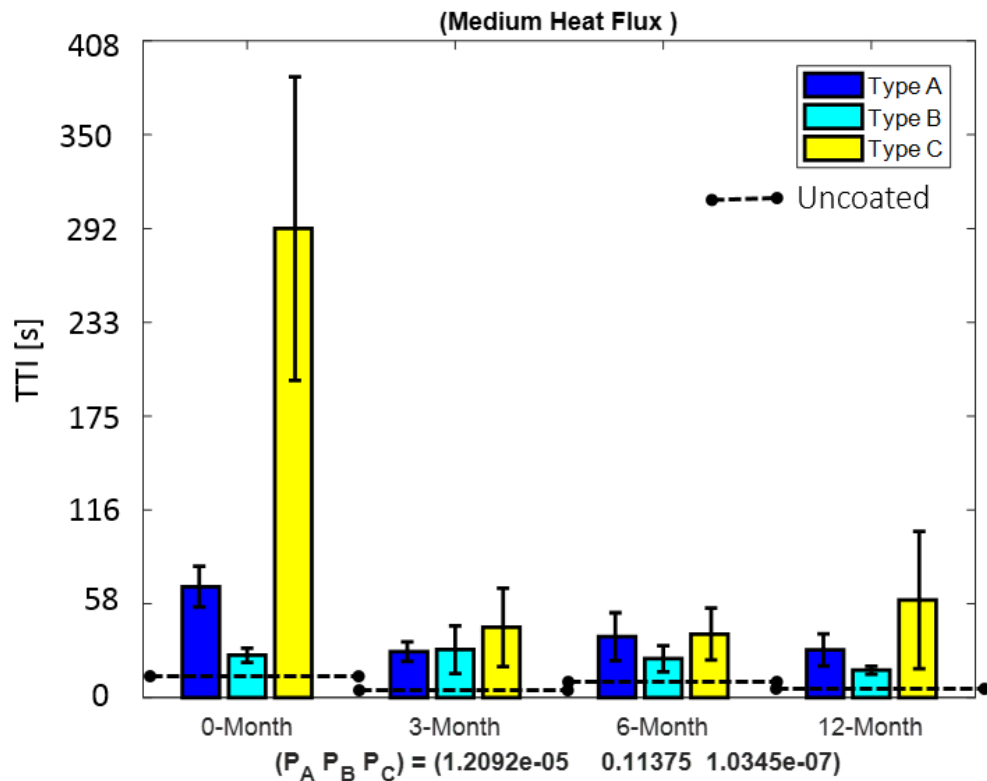


Figure 25: Effect of weathering on TTI in low heat flux test

Figure 25 shows the weathering effects on the TTI in medium heat flux tests on coated samples. The four dashed lines in the graph show the base lines (the mean value of TTI in uncoated specimens) in different weathering durations. The corresponding values in low heat flux show that the maximum TTI recorded in medium heat flux tests was only 68% of the maximum TTI observed in low heat flux tests. The effect of the weathering on measured TTI was presented in P-values beneath the graph in Figure 25. The P-values for type A and C showed the rejection of null hypotheses. In these cases, distinct shifts in the average response variable of TTI were clear. Therefore, weathering was effective on type A and C. As seen in Figure

25, TTI is getting shorter by weathering in these two types. On the other hand, the calculated P-value for type B did not show a severe effect of weathering on the performance of this type. However, the protection established by type B was very poor before weathering.

Table 14: Change in average of TTI in second because of coating in medium heat flux tests.

	0-Month	3-Month	6-Month	12-Month
Type A	49.33	16.83	23.16	20.83
Type B	6.66	18.16	9.50	8.16
Type C	272.33	32.00	24.83	51.83

Table 15: P-values comparing performance of coated from uncoated counterparts in TII under medium heat flux.

	0-Month	3-Month	6-Month	12-Month
Type A	0.0000	0.0001	0.0041	0.0006
Type B	0.0060	0.0151	0.0250	0.0001
Type C	0.0000	0.0098	0.0041	0.0141

In Table (14), the shifts in TTI of coating specimens from uncoated counterparts are listed. The positive values show that TTI in coated samples were longer than the uncoated counterpart. However, the type B protection was much poorer than the other types. The recorded TTI for type A was 8 times longer than type B. However, the performance of type A dramatically dropped during 3 months of weathering. The performance of type A was not better than type B. The same behavior was observed in type C. The weathering effects decreased the TTI just after 3 months.

The P-values of comparing the coated specimens to the uncoated counterparts are listed in Table (15). The rejection of null hypothesis confirmed that the shifts in TTI

are repeatable, and coating can be considered as an effective treatment to increase TTI even in 12 months weathered samples.

4.2.2 HRR in Medium Heat Flux Test

The measured HRR for coated samples and effect of weathering are presented in Figure 26. The four dashed lines in the graph show the base lines (the mean value of HRR in uncoated specimens) in different weathering durations. The P-values of the effect of weathering on each type of coating are listed under the graph in Figure 26.

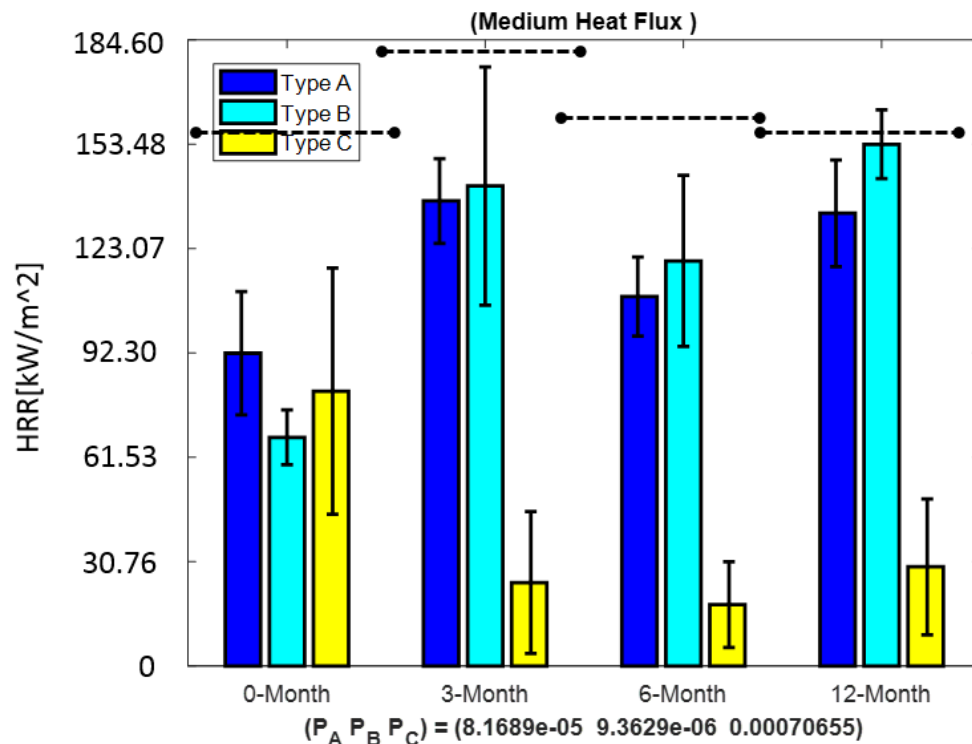


Figure 26: Effect of weathering on HRR in medium heat flux test

All the P-values rejected the null hypothesis. This means that weathering affected the HRR of coating in all three different types. However, the weathering effects were different for type C. As shown in Figure 26, the HRR decreased by weathering for type

C, despite the behavior observed in type A and B. The same behavior was observed in low heat flux tests.

Table 16: Change in average of HRR in kW/m^2 because of coating in medium heat flux tests.

	0-Month	3-Month	6-Month	12-Month
Type A	-69.67	-46.36	-59.77	-24.25
Type B	-94.47	-41.95	-49.23	-3.91
Type C	-80.87	-158.89	-150.56	-128.50

Table 17: P-values comparing performance of coated from uncoated counterparts in HRR under medium heat flux.

	0-Month	3-Month	6-Month	12-Month
Type A	0.0001	0.0001	0.0000	0.0203
Type B	0.0000	0.0201	0.0012	0.6040
Type C	0.0007	0.0000	0.0000	0.0000

In Table (16), the shifts in HRR of coated specimens from the uncoated counterparts are listed. The negative values show that in all cases, the HRR of coated samples were greater than coated counterparts.

In Table (17), the P-values of comparing coated and uncoated samples in HRR in medium heat flux tests are listed. All the P-values rejected null hypothesis, meaning the coating was an effective treatment to decrease HRR. The only exception was found in type B in 12 months weathering. In this case, the HRR of coated samples is not much better than uncoated counterparts. Type A and C showed protection even after 12 months of weathering. In the case of type C, the performance was improved by weathering.

4.2.3 MLR in Medium Heat Flux Test

The effect of weathering on MLR in medium heat flux test was studied. The MLR in different time of weathering for three type of coating is shown in Figure 27. The four dashed lines in the graph show the base lines (the mean value of MLR in uncoated specimens) in different weathering durations. The P-values of the effect of weathering on each coating type is displayed below the graph.

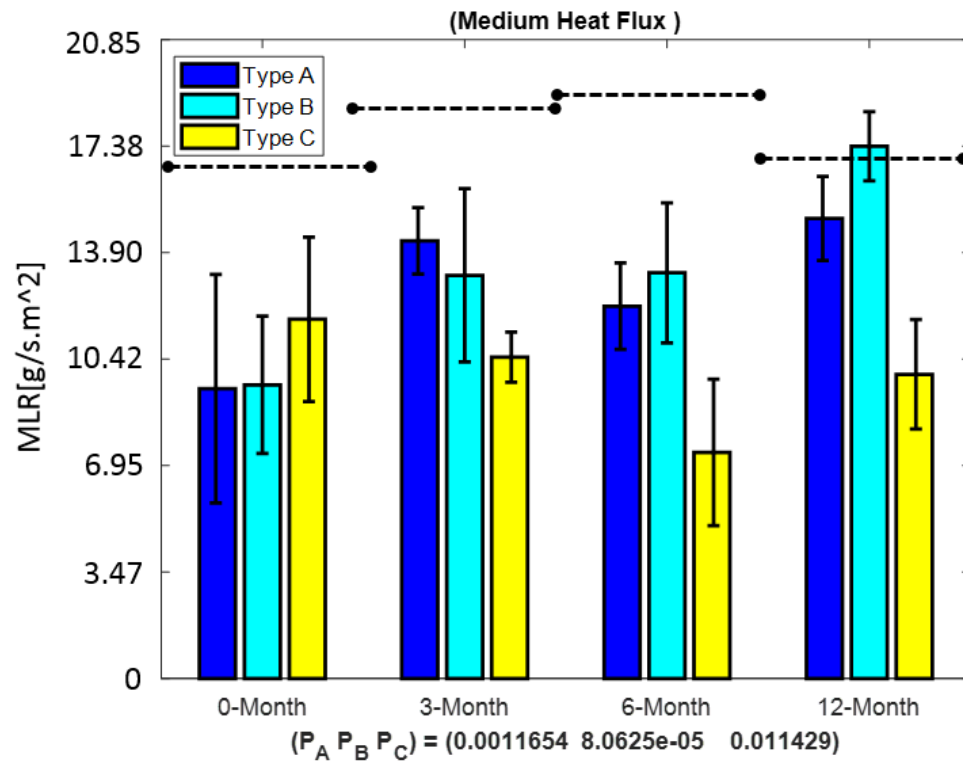


Figure 27: Effect of weathering on MLR in medium heat flux test

The reported P-values for all types of coating showed that the weathering was effective on the performance of the coatings. However, the effects of weathering were not in the same way for all types. In the case of type C, MLR was decreased by weather-

ing time. In the other cases (A and B), weathering effects increased the MLR. The performance of type C was getting better by weathering, while the performance of type A and B were getting poorer due to weathering process.

Table 18: Change in average of MLR in $gr/s.m^2$ because of coating in medium heat flux tests.

	0-Month	3-Month	6-Month	12-Month
Type A	-7.48	-4.35	-7.44	-1.79
Type B	-7.36	-5.47	-6.35	0.56
Type C	-5.22	-8.14	-12.21	-6.88

Table 19: P-values comparing performance of coated from uncoated counterparts in MLR under medium heat flux.

	0-Month	3-Month	6-Month	12-Month
Type A	0.0009	0.0000	0.0000	0.1246
Type B	0.0000	0.0013	0.0001	0.5895
Type C	0.0017	0.0000	0.0000	0.0002

In Table (18), the shifts from the MLR of uncoated samples are listed. The negative values show that the MLR in coated samples were less than uncoated counterparts. The only exception was type B/12-Month. In this case, the MLR of the uncoated sample is less than coated counterparts.

The P-values of comparing coated and uncoated MLR are listed in Table (19). All P-values rejected null hypothesis except type A and B/12-Month. The statistical results showed no evidence supporting the advantage of using these two types of coating in the 12-month weathered samples.

4.2.4 EHC in Medium Heat Flux Test

The average of EHC results is plotted in Figure 28. The four dashed lines in the graph show the base lines (the mean value of EHVC in uncoated specimens) in different weathering durations. The P-values of the weathering effects on EHC for each type are listed below the graph. The P-values showed that weathering affected the EHC. The interesting behavior of decreasing of EHC by weathering was seen in all type of coatings. It means the performance of coating improved by weathering.

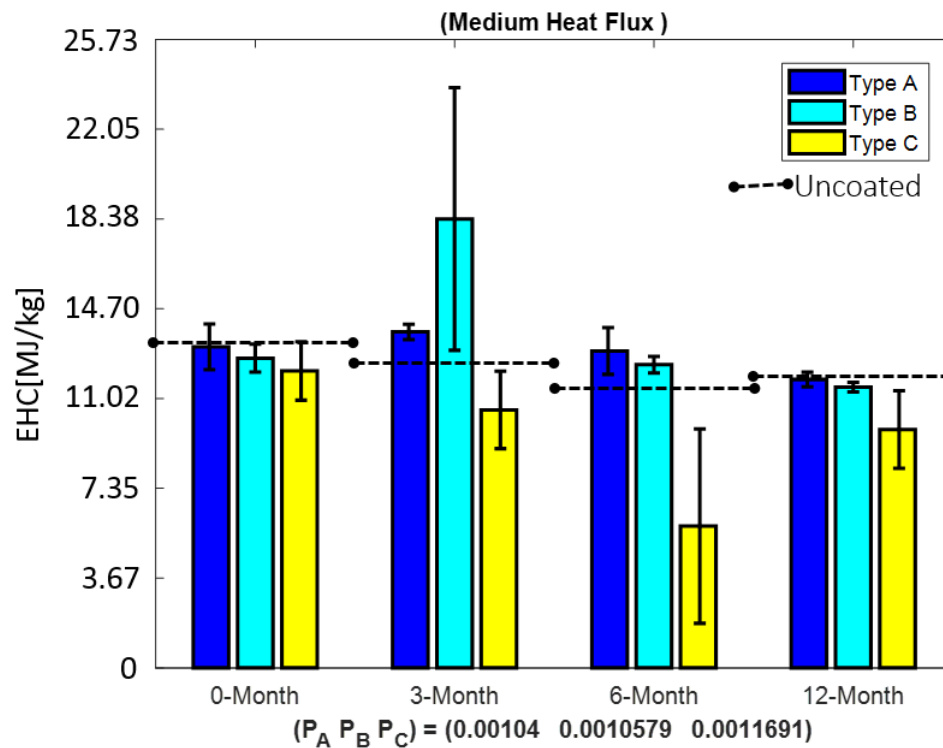


Figure 28: Effect of weathering on EHC in medium heat flux test

In the next step, the shifts in average EHC of specimens from the uncoated counterparts were calculated. The results are listed in Table (20). The positive values depict that the EHC of coated specimen was greater than the uncoated counterparts. The negative values were seen in all type of coatings. It is important to recall that

material with less EHC produces less heat in combustion. It seems that there was a natural process that decreasing EHC of the specimens in respect to time.

The P-values of comparing coated with uncoated counterparts are listed in Table (21). In three cases, the null hypotheses were confirmed. P-values of these cases are remarked by bold font.

Table 20: Change in average of EHC in MJ/kg due to coating under medium heat flux tests.

	0-Month	3-Month	6-Month	12-Month
Type A	-0.23	1.17	1.33	-0.32
Type B	-0.69	5.79	0.77	-0.63
Type C	-1.21	-2.02	-5.83	-2.37

Table 21: P-values comparing performance of coated from uncoated counterparts in EHC under medium heat flux.

	0-Month	3-Month	6-Month	12-Month
Type A	0.6073	0.0002	0.0101	0.2278
Type B	0.0552	0.0250	0.0044	0.0217
Type C	0.0464	0.0128	0.0050	0.0060

4.3 High Heat Flux Test

The weathering effects on the results of high heat flux tests ($70 \text{ kW}/\text{m}^2$) is presented in this section. In real fire, the exposure time of high heat flux can be very short [101], however the damage of high heat flux can be enormous due to high concentration of heat energy on the surface of structures.

4.3.1 TTI in High Heat Flux Test

The effect of weathering on TTI in high heat flux tests is shown in Figure 29. The P-values of the weathering effects for each type of coating are listed below the

graph. The four dashed lines in the graph show the base lines (the mean value of TTI in uncoated specimens) in different weathering durations. The maximum TTI recorded for high heat flux test was 13% and 9% of the maximums of TTI reported for medium and low heat flux tests. In all cases, the P-values rejected the null hypothesis.

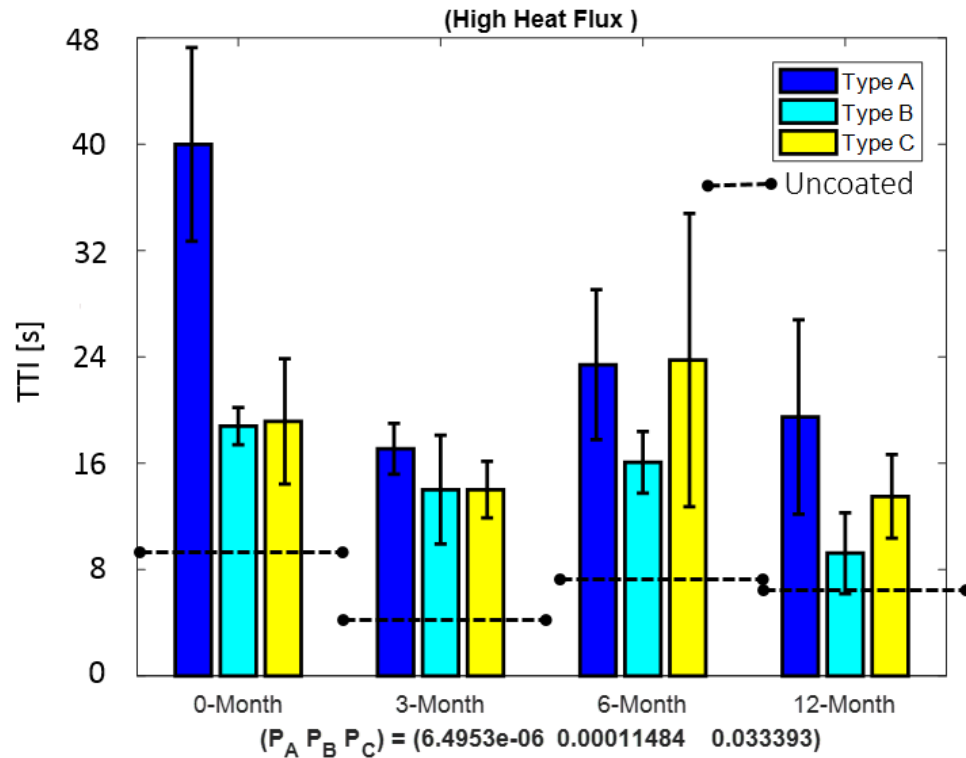


Figure 29: Effect of weathering on MLR in medium heat flux test

The TTI of the samples were getting shorter by weathering. Type A showed the best performance before the weathering process. However, the performance of the A coated sample extensively decreased just after 3 months of the natural weathering. The average TTI in 3-month data for type A was almost half its initial value before the effects of weathering.

In the next step, the advantage of the coating was studied. In Table (22), the shifts

Table 22: Change in average of TTI in second because of coating in high heat flux tests.

	0-Month	3-Month	6-Month	12-Month
Type A	29.33	11.83	16.00	12.50
Type B	8.66	8.83	8.83	2.50
Type C	9.00	8.83	16.33	6.66

Table 23: P-values comparing performance of coated from uncoated counterparts in TTI under high heat flux.

	0-Month	3-Month	6-Month	12-Month
Type A	0.0000	0.0000	0.0000	0.0016
Type B	0.0000	0.0005	0.0000	0.0750
Type C	0.0010	0.0000	0.0041	0.0004

in TTI of coated specimens from uncoated counterparts are listed. The positive values mean that in all cases, the TTI increased by coating. The P-values of the comparison TTI of coated and uncoated are listed in Table (23). In all cases, the repeatability of improvement confirmed except type B/12-Month. It is the only case where there was no statistical evidence that coating performed better than uncoated samples in high heat flux tests.

4.3.2 HRR in High Heat Flux Test

The weathering effects on HRR in high heat flux was analyzed. The HRR in high heat flux tests is shown in Figure 30. The four dashed lines in the graph show the base lines (the mean value of HRR in uncoated specimens) in different weathering durations. The P-values showing effect of weathering are listed below the graph. In high heat flux test, the P-values of type A and B rejected the null hypothesis. It means that weathering caused a shift in the average of HRR in these two types. The bars in Figure 30 show that the measured HRR increased by weathering.

In the case of type C, the P-value confirmed the null hypothesis. It means there was no statistical evidence that weathering was effective on the performance of type C. Moreover, the measured HRR for samples coated by type C was much smaller.

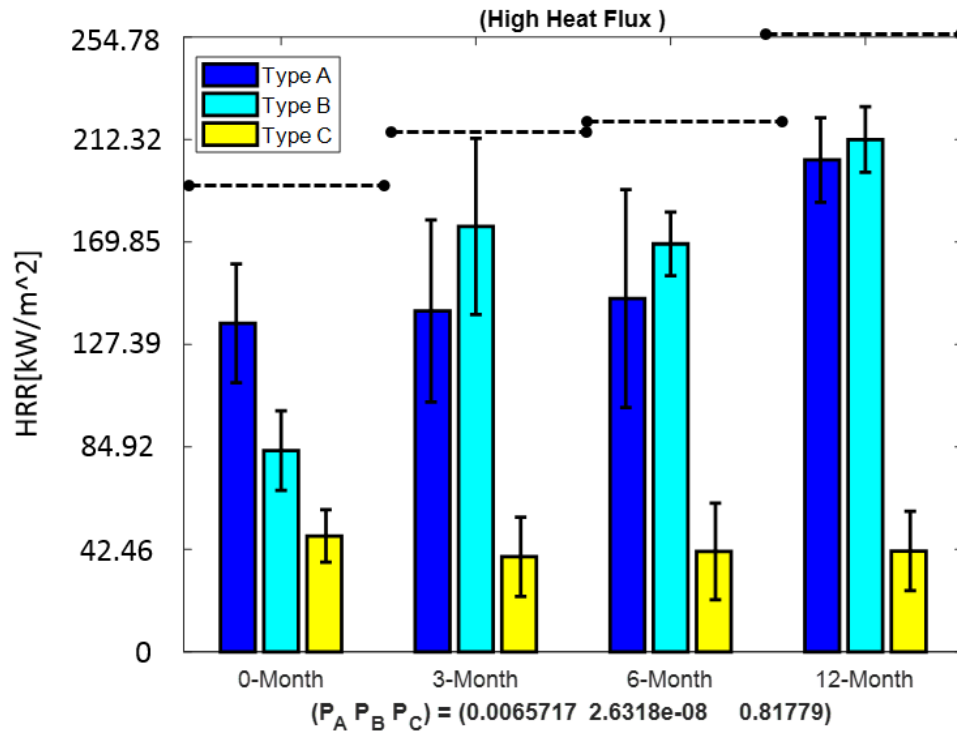


Figure 30: Effect of weathering on HRR in high heat flux test

In the next step, the effects of coating was investigated. The coated specimens and uncoated counterparts were compared. The shifts in the average of measured HRR of coated specimens from uncoated counterparts are listed in Table (24). The negative sign of reported numbers shows that in all cases, the HRR of coated samples were less than uncoated counterparts. It is important to notice that the magnitude of the shift in average HRR for the samples coated with type C was much greater than two other types. It displayed the advantage of type C over the other tested types due to decreasing HRR in high heat flux tests.

Table 24: Change in average of HRR in kW/m^2 because of coating in high heat flux tests.

	0-Month	3-Month	6-Month	12-Month
Type A	-57.74	-78.00	-77.82	-55.64
Type B	-111.49	-42.93	-55.16	-47.19
Type C	-146.89	-179.82	-182.58	-217.72

Table 25: P-values comparing performance of coated from uncoated counterparts in HRR under high heat flux.

	0-Month	3-Month	6-Month	12-Month
Type A	0.0043	0.0033	0.0042	0.0001
Type B	0.0000	0.0571	0.0007	0.0001
Type C	0.0000	0.0000	0.0000	0.0000

The P-values of the checking the effect of the coating are listed in Table (25). All the P-values rejected null hypothesis except type B/3-Month. It means in almost all cases, the coating is an effective treatment to decrease the HRR.

4.3.3 MLR in High Heat Flux Test

The MLR in high heat flux tests was analyzed. The results are shown in Figure 31. The four dashed lines in the graph show the base lines (the mean value of MLR in uncoated specimens) in different weathering durations. The P-values calculated for effects of weathering on MLR are listed below the graph in Figure 31. The P-values for type A and B rejected the null hypothesis. It means that weathering changed the MLR in the specimens coated with type A and B. As displayed by the bar charts in Figure 31, the MLR was getting higher by weathering. The results from type C was different, the P-value for type C confirmed the null hypothesis. There was no statistical evidence that MLR in specimens coated with type C was affected by weathering.

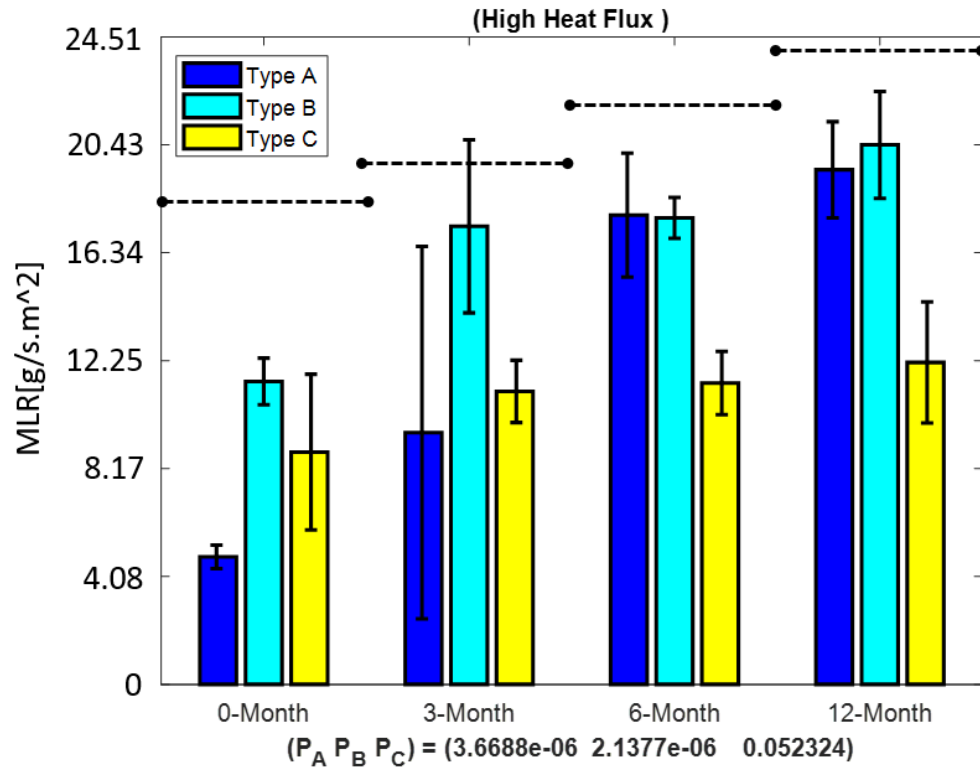


Figure 31: Effect of weathering on MLR in high heat flux test

The analysis between coated specimens and uncoated counterparts can show the advantage of the coating. The shifts of average MLR of coated specimens from the uncoated counterparts are listed in Table (26). The negative values demonstrate that in all cases, the MLR of coated specimens were less than uncoated counterparts.

Table 26: Change in average of MLR because of coating in high heat flux tests.

	0-Month	3-Month	6-Month	12-Month
Type A	-13.17	-10.41	-4.80	-4.52
Type B	-6.52	-2.60	-4.90	-3.58
Type C	-9.20	-8.85	-11.15	-11.82

In the next step, the P-values of the comparisons between coated and uncoated specimens were calculated. The results are listed in Table (27). All the P-values rejected null hypothesis. It means that all the shifts in average MLR were repeatable

Table 27: P-values comparing performance of coated from uncoated counterparts in MLR under high heat flux.

	0-Month	3-Month	6-Month	12-Month
Type A	0.0000	0.0072	0.0142	0.0002
Type B	0.0003	0.1699	0.0045	0.0024
Type C	0.0002	0.0000	0.0000	0.0000

results. The only exception was in type B/3-Month. The same behavior was seen in HRR data in high heat flux tests.

4.3.4 EHC in High Heat Flux Test

The average of EHC results is plotted in Figure 32. The four dashed lines in the graph show the base lines (the mean value of EHC in uncoated specimens) in different weathering duration. The P-values of the weathering effects on EHC for each type are listed below the graph. The P-values showed that weathering affected the EHC. The interesting behavior of decreasing of EHC by weathering was seen in all types of the coatings. Meaning the performance of the coating in EHC was improved by weathering.

In the next step, the shift in average EHC of specimens from the uncoated counterparts was calculated. The results are listed in Table (28). The positive values show that the EHC of coated specimen was greater than uncoated counterparts. The negative values were seen in all types. It is important to recall that material with less EHC produces less heat energy in combustion. It seems that there was a natural process of decreasing EHC of the specimens with respect to time.

The P-values of comparing coated with uncoated counterparts are listed in Table (29). In four cases, the null hypotheses were confirmed. These P-values are remarked

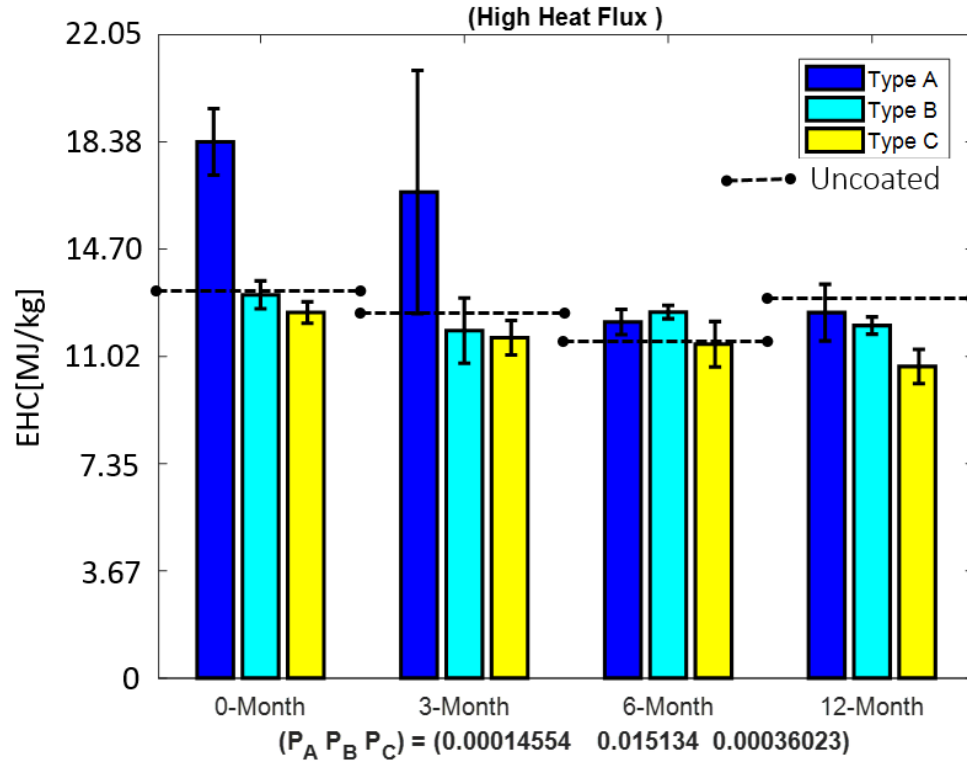


Figure 32: Effect of weathering on EHC in high heat flux test

by bold font.

Table 28: Change in average of EHC in MJ/kg because of coating in high heat flux tests.

	0-Month	3-Month	6-Month	12-Month
Type A	5.02	4.02	0.59	-0.36
Type B	-0.22	-0.72	0.93	-0.80
Type C	-0.82	-0.97	-0.16	-2.20

4.4 Overview of Coating Performance

In this section, the summary of the performance of coatings during the process of weathering is presented. The performance of uncoated counterparts was selected as the reference of the analogy. In the cases where the performance of coated specimens was not statistically better than uncoated counterparts, it was assumed that there is

Table 29: P-values comparing performance of coated from uncoated counterparts in EHC under high heat flux.

	0-Month	3-Month	6-Month	12-Month
Type A	0.0000	0.0404	0.0124	0.3952
Type B	0.4135	0.1616	0.0000	0.0003
Type C	0.0044	0.0066	0.6328	0.0000

no advantage of coating anymore. In some cases, there was the statistical evidence of better performance of coated specimens, however, these advantages were insignificant in comparing with other types of coating. The information can be used to determine the renewing time for each of the coating type.

4.4.1 Overview Over TTI of Coated Specimens

The effect of weathering on TTI of coated specimens is shown in Figure 33. The black solid boxes display the places that the performance of the coated samples was relatively significant. In cases of type A and C coatings, the coating showed an effective protection which can be seen even in 12-month weathered samples. In type B, lack of affection was seen even before starting the process of weathering in medium heat flux tests results. The same poor performance was seen during the process of weathering. In the 12-month weathering, type B did not show any statistical evidence of protection in measured TTI of the samples.

Time to Ignition												
	0 Month			3 Month			6 Month			12 Month		
Type A	Low	Med	High	Low	Med	High	Low	Med	High	Low	Med	High
Type B	Low	Med	High	Low	Med	High	Low	Med	High	Low	Med	High
Type C	Low	Med	High	Low	Med	High	Low	Med	High	Low	Med	High

Figure 33: Effect of weathering on TTI

4.4.2 Overview Over HRR of Coated Specimens

The effect of weathering on HRR of coated specimens is shown in Figure 34. The black solid boxes show the places that the performance of coated samples was relatively significant. Type C displayed the best performance. In all samples coated with type C, the decreasing of HRR was seen. In type A, with only one exception (12-Month/Low heat flux test), the decreasing in HRR was observed. However, the magnitude of the decreasing measured HRR from type C was much greater than type A. In the case of type B, the sign of degradation appeared in 3-month weathering data. In the 12 months of weathering, the advantage of the coating of type B disappeared. The average HRR for B-coated/12-month weathered specimens was even higher than uncoated samples in low heat flux tests.

Heat Release Rate												
	0 Month			3 Month			6 Month			12 Month		
Type A	Low	Med	High	Low	Med	High	Low	Med	High	Low	Med	High
Type B	Low	Med	High	Low	Med	High	Low	Med	High	Low	Med	High
Type C	Low	Med	High	Low	Med	High	Low	Med	High	Low	Med	High

Figure 34: Effect of weathering on HRR

4.4.3 Overview Over MLR of Coated Specimens

The effect of weathering on MLR of coated specimens is shown in Figure 35. The black solid boxes show the places that the performance of coated samples was relatively significant. Type C depicted the best performance. In all samples coated with type A and C, the decreasing of MLR was seen. However, the magnitude of decrease-

ing of measured MLR with type C was much greater than type A. In the case of B, the sign of degradation appeared in 3-month weathering data. In the 12 months of weathering, the advantage of the coating of type B disappeared. The average MLR for B-coated/12-month weathered specimens was even higher than uncoated samples in medium heat flux tests.

Mass Loss Rate												
	0 Month			3 Month			6 Month			12 Month		
Type A	Low	Med	High	Low	Med	High	Low	Med	High	Low	Med	High
Type B	Low	Med	High	Low	Med	High	Low	Med	High	Low	Med	High
Type C	Low	Med	High	Low	Med	High	Low	Med	High	Low	Med	High

Figure 35: Effect of weathering on MLR

4.4.4 Overview Over EHC of Coated Specimens

It seems that there is a natural process occurring which decreased the EHC. This parameter improved in all cases by weathering.

4.4.5 Overview Over Ignition Probability

Based on results presented in Table (2), the maximum duration of heat flux measured in real fires in each level of low, medium and high were reported as 145 second, 60 second and 8 second. These values in comparison with the average TTI measured for each class showed low and medium heat fluxes could be more devastating for coating treatment than high heat flux. All classes except one class (B-type/12-month) could survive the high heat flux duration without ignition. The medium heat flux results for TTI showed the most extreme situation for coating treatments. In medium

heat flux, all classes could not survive without ignition except one class (type C/0-Month). In low heat flux, natural weathering just after 3 months destroyed the chance of surviving in A and B types against ignition. The results showed minor chance for type C to be survived without ignition.

4.5 Critical Heat Flux

As mentioned in section (3.3), there are several theoretical models used to calculate critical heat flux (q''_{cr}). Two models were discussed: thermally thick and thermally thin solid models. These models were employed to calculate the critical heat flux. The results of the two models are listed in Tables (30, 31).

Table 30: Critical heat fluxes based on thermally thick solid model.

	0-Month	3-Month	6-Month	12-Month
Uncoated	11.4 (kW/m^2)	12.2 (kW/m^2)	11.8 (kW/m^2)	5.2 (kW/m^2)
Type A	9.2 (kW/m^2)	6.4 (kW/m^2)	0.0 (kW/m^2)	-10.2 (kW/m^2)
Type B	17.5 (kW/m^2)	2.5 (kW/m^2)	-4.3 (kW/m^2)	6.1 (kW/m^2)
Type C	25.8 (kW/m^2)	19.9 (kW/m^2)	11.9 (kW/m^2)	25.2 (kW/m^2)

Table 31: Critical heat fluxes based on thermally thin solid model.

	0-Month	3-Month	6-Month	12-Month
Uncoated	25.6 (kW/m^2)	27.3 (kW/m^2)	26.0 (kW/m^2)	20.7 (kW/m^2)
Type A	23.7 (kW/m^2)	22.8 (kW/m^2)	19.2 (kW/m^2)	14.4 (kW/m^2)
Type B	25.6 (kW/m^2)	22.0 (kW/m^2)	17.0 (kW/m^2)	22.1 (kW/m^2)
Type C	34.1 (kW/m^2)	30.1 (kW/m^2)	24.6 (kW/m^2)	32.7 (kW/m^2)

There are some important points about the results presented in Tables (30, 31). First, the negative values and zero, shown in bold font in Table (30) , are not reasonable for critical heat flux of the specimens. This may be a sign that the thermally thick solid model was not an appropriate model for the specimens with the nominal

thickness of 12.5 mm under the effective heat flux above 30 kW/m^2 . It seems that the thermally thin solid model was a better theory to calculate the critical heat fluxes for the specimens (see Table (31)). At least, there is no negative or zero value calculated for critical heat flux in this model. Second, the critical heat flux for almost all specimens coated with type C, listed in Table (31), was greater than the counterparts coated with other types. This means the performance of type C was relatively better. Thirdly, there are two concerns about the accuracy of the results. The assumption of no phase change in the calculation of surface temperature is not valid when the samples were coated with intumescent fire retardant materials. The phase change occurs in the heating these materials. In order to calculate the critical heat flux relatively accurate, TTI in several effective heat fluxes are required. In this study, only TTI of three different effective heat fluxes were available (TTI of 30, 50 and 70 kW/m^2).

CHAPTER 5: CONCLUSION

5.1 Conclusion Result

In regards to the first concern: overall, weathering exposure decreased the effectiveness of fire protection of intumescent coatings. This fact was more clear in the study of TTI. Degradations in coatings was observed in all three types. However, some types can preserve their protection for a longer time. In type C, the measured HRR showed improvement by weathering. Type C was a water-based intumescent coating. The type C coating was the thickest dry film after coating over the specimens. As mentioned in chapter two, the water solubility was measured to find the optimized intumescent coating. However, The results showed that the thickness of the dry layer or number of layers could also play a role in weathering resistance of the intumescent coating.

Pertaining to the second concern: EHC seemed more affected by weathering than the coatings. The coated samples and uncoated counterparts showed almost close value of EHC. In all cases, EHC decreased or stayed almost fixed by weathering process. However, increasing in the performance of other combustion properties was not seen in almost all weathered specimens coated with type A, B and C. There was only two cases where the combustion properties of the coated samples was worse than the uncoated counterparts (MLR B-type/Medium HF/12-Month and HRR B-type/low

HF/12-Month).

Heat flux levels had a huge impact on the fire protection effectiveness of coatings. Selection of the intumescent type based on heat flux risk can be considered important. Therefore, information on heat flux range would be helpful for consumers of these intumescent coatings. The result in TTI displayed showed that the medium heat flux in real fire imposed the most extreme condition on coating treatments. Weathering orientation demonstrated much less effect on the performance of the intumescent coatings in comparison to the other parameters.

Note: Testing and data analysis were done on the weathered specimens from only one location (Richburg, SC) and they were exposed to the weathering effects for one year.

5.2 Significant of Research

Impregnated and intumescent coating are widely used in fire protection of wooden structures. The general application of intumescent coatings exposes the coating to a higher risk of weathering. It was the lack of standard procedure establishment for application of the coatings on wooden substrates. The first step to establishing such a standards is the better understanding of effects of weathering on performance for these materials.

This project was following a comprehensive study funded by IBHS focused on the weathering effects on the intumescent coating. In most of related researches, the natural weathering, which is a time consuming process, has been replaced by arti-

ficial weathering techniques. It is important to notice that the artificial weathering techniques can not be considered as a comprehensive approach. As an example the biological factors in a natural process of weathering was ignored or reduced in most of these techniques. It was found that the weathering affected noticeably the performance of this type of coating. In one of the cases, the performance of coating almost disappeared in less than one year.

The information of such studies may lead to a standard which optimizes the fire protection provided by intumescent coating.

5.3 Recommendation for Future Research

Two types (type A and C) out of three tested types of the intumescent coatings performed better than uncoated samples in 12 months of weathering. However, the advantage of using type A was just marginal after 12 months weathering. The project could continue only by testing the performance of type C.

Lack of comprehensive theoretical model of burning woods paralyzes the results. It seems the transition state theory has a promising potential to explain burning fuel. Wood, in general, is the combination of several fuels with different activation energies. Lignin and Cellulose are two of the main fuels in wood. In all HRR graphs from calorimetry, two peaks were seen. These peaks can be sign as the participation of each of these two fuels in the burning process. The advantage of transition state theory is in the involving parameters which do not generally depend on the effective heat flux. In most of cases, there is lack of information of effective heat flux in real fires.

The transition state theory provides a theoretical understanding of the chemical reactions rate [108]. Based on this theory, a quasi-equilibrium between reactants and activated complexes exists.



Where A and B are the reactants, and $[AB]^*$ is the concentration of activated complex. The theory conducted to predict MLR and HRR of heated surfaces [109].

One future research can be the expansion of the transition state theory for two fuels in wood. Then fitting experimental curves of HRR and MLR to theoretical ones can provide an estimation of activation energy for each case. The results of such an analysis can determine the effects of weathering or coatings on activation energy, which plays an important role in combustion properties of samples in all effective heat fluxes.

Another useful research that can be considered as complementary to this project is the investigation on the mean of fire propagations. Understanding the mechanism of firebrands in the propagation of fires is one type of potential research topic. The level of heat flux risk could provide useful information to users of intumescent coating.

Bibliography

- [1] Babak Bahrani. Effects of weathering on performance of intumescent coatings for structure fire protection in the wildland-urban interface. Master's thesis, The University of North Carolina at Charlotte, 2015.
- [2] René Delobel, Michel Le Bras, Najib Ouassou, and Fatia Alistiqsa. Thermal behaviours of ammonium polyphosphate-pentaerythritol and ammonium pyrophosphate-pentaerythritol intumescent additives in polypropylene formulations. *Journal of Fire Sciences*, 8(2):85–108, 1990.
- [3] S Duquesne and T Futterer. Intumescent systems. *Non-Halogenated Flame Retardant Handbook*, pages 293–346, 2014.
- [4] HL Vandersall. Intumescent coating systems, their development and chemistry. *Journal of Fire and Flammability*, 2(2):97–140, 1971.
- [5] Serge Bourbigot, Michel Le Bras, Sophie Duquesne, and Maryline Rochery. Recent advances for intumescent polymers. *Macromolecular Materials and Engineering*, 289(6):499–511, 2004.
- [6] PJ Longdon, C Houyoux, B Zhao, and B Chico. Development of alternative technologies for off-site applied intumescent coatings. *EUR*, (21216):1–141, 2005.
- [7] René Delobel, Najib Ouassou, Michel Le Bras, and Jean-Marie Leroy. Fire retardance of polypropylene: Action of diammonium pyrophosphate-pentaerythritol intumescent mixture. *Polymer degradation and stability*, 23(4):349–357, 1989.
- [8] Deng-Hui Wu, Pei-Hua Zhao, Ya-Qing Liu, Xue-Yi Liu, and Xiao-feng Wang. Halogen free flame retardant rigid polyurethane foam with a novel phosphorus-nitrogen intumescent flame retardant. *Journal of Applied Polymer Science*, 131(11), 2014.
- [9] Lei Shi, Zhong-Ming Li, Bang-Hu Xie, Jian-Hua Wang, Chun-Rong Tian, and Ming-Bo Yang. Flame retardancy of different-sized expandable graphite particles for high-density rigid polyurethane foams. *Polymer international*, 55(8):862–871, 2006.
- [10] DM Hwang, G Kirczenow, P Lagrange, A Magerl, R Moret, SC Moss, S Setton, SA Solin, Hartmut Zabel, and Stuart A Solin. *Graphite Intercalation Compounds I: Structure and Dynamics*, volume 14. Springer Science & Business Media, 2013.
- [11] G Camino, S Duquesne, R Delobel, B Eling, C Lindsay, and T Roels. Mechanism of expandable graphite fire retardant action in polyurethanes. In *ABSTRACTS OF PAPERS OF THE AMERICAN CHEMICAL SOCIETY*, volume 220, pages U333–U334. AMER CHEMICAL SOC 1155 16TH ST, NW,

WASHINGTON, DC 20036 USA, 2000.

- [12] Giovanni Camino, L Costa, and L Trossarelli. Study of the mechanism of intumescence in fire retardant polymers: Part iii—effect of urea on the ammonium polyphosphate-pentaerythritol system. *Polymer Degradation and Stability*, 7(4):221–229, 1984.
- [13] Giovanni Camino, L Costa, and L Trossarelli. Study of the mechanism of intumescence in fire retardant polymers: Part ii—mechanism of action in polypropylene-ammonium polyphosphate-pentaerythritol mixtures. *Polymer Degradation and Stability*, 7(1):25–31, 1984.
- [14] Giovanni Camino, L Costa, L Trossarelli, F Costanzi, and A Pagliari. Study of the mechanism of intumescence in fire retardant polymers: Part vi—mechanism of ester formation in ammonium polyphosphate-pentaerythritol mixtures. *Polymer Degradation and Stability*, 12(3):213–228, 1985.
- [15] Serge Bourbigot, Michel Le Bras, and René Delobel. Carbonization mechanisms resulting from intumescence association with the ammonium polyphosphate-pentaerythritol fire retardant system. *Carbon*, 31(8):1219–1230, 1993.
- [16] Serge Bourbigot, Michel Le Bras, Léon Gengembre, and René Delobel. Xps study of an intumescent coating application to the ammonium polyphosphate/pentaerythritol fire-retardant system. *Applied surface science*, 81(3):299–307, 1994.
- [17] René Delobel, Najib Ouassou, Michel Le Bras, and Jean-Marie Leroy. Fire retardance of polypropylene: Action of diammonium pyrophosphate-pentaerythritol intumescent mixture. *Polymer degradation and stability*, 23(4):349–357, 1989.
- [18] Bernhard Schartel, Uta Knoll, Andreas Hartwig, and Dirk Pütz. Phosphonium-modified layered silicate epoxy resins nanocomposites and their combinations with ath and organo-phosphorus fire retardants. *Polymers for advanced technologies*, 17(4):281–293, 2006.
- [19] Shih-Hsuan Chiu and Wun-Ku Wang. Dynamic flame retardancy of polypropylene filled with ammonium polyphosphate, pentaerythritol and melamine additives. *Polymer*, 39(10):1951–1955, 1998.
- [20] Giovanni Camino, L Costa, and L Trossarelli. Study of the mechanism of intumescence in fire retardant polymers: Part v—mechanism of formation of gaseous products in the thermal degradation of ammonium polyphosphate. *Polymer Degradation and Stability*, 12(3):203–211, 1985.
- [21] Igor S Reshetnikov, Anatoly N Garashchenko, and Valery L Strakhov. Experimental investigation into mechanical destruction of intumescent chars. *Polymers for Advanced Technologies*, 11(8-12):392–397, 2000.

- [22] S Duquesne, R Delobel, M Le Bras, and Giovanni Camino. A comparative study of the mechanism of action of ammonium polyphosphate and expandable graphite in polyurethane. *Polymer degradation and stability*, 77(2):333–344, 2002.
- [23] M Jimenez, S Duquesne, and S Bourbigot. Characterization of the performance of an intumescent fire protective coating. *Surface and coatings Technology*, 201(3):979–987, 2006.
- [24] Maryska Muller, Serge Bourbigot, Sophie Duquesne, Rene A Klein, Giacomo Giannini, and Chris I Lindsay. Measurement and investigation of intumescent char strength: Application to polyurethanes. *Journal of Fire Sciences*, page 0734904112472015, 2013.
- [25] Charles E Anderson, Donald E Ketchum, William P Mountain, et al. Thermal conductivity of intumescent chars. *Journal of Fire Sciences*, 6(6):390–410, 1988.
- [26] JEJ Staggs. Thermal conductivity estimates of intumescent chars by direct numerical simulation. *Fire Safety Journal*, 45(4):228–237, 2010.
- [27] Ya Zhang, YC Wang, CGa Bailey, and AP Taylor. Global modelling of fire protection performance of intumescent coating under different cone calorimeter heating conditions. *Fire Safety Journal*, 50:51–62, 2012.
- [28] Robert J Asaro, Brian Lattimer, Chris Mealy, and George Steele. Thermo-physical performance of a fire protective coating for naval ship structures. *Composites Part A: Applied Science and Manufacturing*, 40(1):11–18, 2009.
- [29] Matthias Bartholmai, Robert Schriever, and Bernhard Schartel. Influence of external heat flux and coating thickness on the thermal insulation properties of two different intumescent coatings using cone calorimeter and numerical analysis. *Fire and materials*, 27(4):151–162, 2003.
- [30] B Gardelle, S Duquesne, V Rerat, and S Bourbigot. Thermal degradation and fire performance of intumescent silicone-based coatings. *Polymers for Advanced Technologies*, 24(1):62–69, 2013.
- [31] LL Wang, YC Wang, JF Yuan, and GQ Li. Thermal conductivity of intumescent coating char after accelerated aging. *Fire and Materials*, 37(6):440–456, 2013.
- [32] Peng Hu, Juan-Juan Yao, and Ze-Shao Chen. Analysis for composite zeolite/foam aluminum–water mass recovery adsorption refrigeration system driven by engine exhaust heat. *Energy Conversion and Management*, 50(2):255–261, 2009.
- [33] Xu Wang, Na Feng, Suqin Chang, Guixia Zhang, Hong Li, and Hongfei Lv. Intumescent flame retardant tpo composites: flame retardant properties and morphology of the charred layer. *Journal of Applied Polymer Science*, 124(3):2071–

2079, 2012.

- [34] M Muller, S Bourbigot, S Duquesne, R Klein, G Giannini, C Lindsay, and J Vlassenbroeck. Investigation of the synergy in intumescent polyurethane by 3d computed tomography. *Polymer degradation and stability*, 98(9):1638–1647, 2013.
- [35] Sven Brehme, Bernhard Schartel, Jürgen Goebbels, O Fischer, D Pospiech, Y Bykov, and M Döring. Phosphorus polyester versus aluminium phosphinate in poly (butylene terephthalate)(pbt): flame retardancy performance and mechanisms. *Polymer Degradation and Stability*, 96(5):875–884, 2011.
- [36] G Montaudo, E Scamporrino, C Puglisi, and D Vitalini. Intumescent flame retardant for polymers. iii. the polypropylene–ammonium polyphosphate–polyurethane system. *Journal of applied polymer science*, 30(4):1449–1460, 1985.
- [37] Michel Bugajny, Michel Le Bras, Serge Bourbigot, Franck Poutch, and Jean-Marc Lefebvre. Thermoplastic polyurethanes as carbonization agents in intumescent blends. part 1: Fire retardancy of polypropylene/thermoplastic polyurethane/ammonium polyphosphate blends. *Journal of fire sciences*, 17(6):494–513, 1999.
- [38] Michel Le Bras, Michel Bugajny, Jean-Marc Lefebvre, and Serge Bourbigot. Use of polyurethanes as char-forming agents in polypropylene intumescent formulations. *Polymer International*, 49(10):1115–1124, 2000.
- [39] X Almeras, F Dabrowski, M Le Bras, F Poutch, S Bourbigot, Gy Marosi, and P Anna. Using polyamide-6 as charring agent in intumescent polypropylene formulations. effect of the compatibilising agent on the fire retardancy performance. *Polymer degradation and stability*, 77(2):305–313, 2002.
- [40] Zhi-Ling Ma, Wei-Yan Zhang, and Xin-Yu Liu. Using pa6 as a charring agent in intumescent polypropylene formulations based on carboxylated polypropylene compatibilizer and nano-montmorillonite synergistic agent. *Journal of applied polymer science*, 101(1):739–746, 2006.
- [41] C Siat, S Bourbigot, and M Le Bras. Structural study of the polymer phases in intumescent pa-6/eva/fr additive blends. *Recent advances in flame retardancy of polymeric materials*, 7(1996):318–326, 1997.
- [42] Fei Xie, Yu-Zhong Wang, Bing Yang, and YA Liu. A novel intumescent flame-retardant polyethylene system. *Macromolecular Materials and Engineering*, 291(3):247–253, 2006.
- [43] Jianqian Huang, Yeqin Zhang, Qi Yang, Xia Liao, and Guangxian Li. Synthesis and characterization of a novel charring agent and its application in intumescent flame retardant polypropylene system. *Journal of Applied Polymer Science*,

- 123(3):1636–1644, 2012.
- [44] Hua-Qiao Peng, Qian Zhou, De-Yi Wang, Li Chen, and Yu-Zhong Wang. A novel charring agent containing caged bicyclic phosphate and its application in intumescent flame retardant polypropylene systems. *Journal of Industrial and Engineering Chemistry*, 14(5):589–595, 2008.
- [45] Kun Yang, Miao-Jun Xu, and Bin Li. Synthesis of n-ethyl triazine–piperazine copolymer and flame retardancy and water resistance of intumescent flame retardant polypropylene. *Polymer degradation and stability*, 98(7):1397–1406, 2013.
- [46] Jiangsong Yi, Yi Liu, Dongdong Pan, and Xufu Cai. Synthesis, thermal degradation, and flame retardancy of a novel charring agent aliphatic–aromatic polyamide for intumescent flame retardant polypropylene. *Journal of Applied Polymer Science*, 127(2):1061–1068, 2013.
- [47] Nana Tian, Xin Wen, Zhiwei Jiang, Jiang Gong, Yanhui Wang, Jian Xue, and Tao Tang. Synergistic effect between a novel char forming agent and ammonium polyphosphate on flame retardancy and thermal properties of polypropylene. *Industrial & Engineering Chemistry Research*, 52(32):10905–10915, 2013.
- [48] Sun Liu, Yi Lun Tan, Si Chun Shao, Yin Yin Hui, and Zhi Han Peng. Synthesis and characterization of a novel polyhydroxy triazine charring agent and properties of its flame retarded polypropylene. In *Advanced Materials Research*, volume 746, pages 23–27. Trans Tech Publ, 2013.
- [49] Menachem Lewin and Makoto Endo. Catalysis of intumescent flame retardancy of polypropylene by metallic compounds. *Polymers for Advanced Technologies*, 14(1):3–11, 2003.
- [50] Ping Wei, Jianwei Hao, Jianxin Du, Zhidong Han, and Jianqi Wang. An investigation on synergism of an intumescent flame retardant based on silica and alumina. *Journal of fire sciences*, 21(1):17–28, 2003.
- [51] X Almeras, M Le Bras, F Poutch, S Bourbigot, G Marosi, and P Anna. Effect of fillers on fire retardancy of intumescent polypropylene blends. In *Macromolecular Symposia*, volume 198, pages 435–448. Wiley Online Library, 2003.
- [52] Hasan Demir, E Arkiş, D Balköse, and S Ülkü. Synergistic effect of natural zeolites on flame retardant additives. *Polymer degradation and stability*, 89(3):478–483, 2005.
- [53] Mehmet Doğan, Aysen Yılmaz, and Erdal Bayramlı. Synergistic effect of boron containing substances on flame retardancy and thermal stability of intumescent polypropylene composites. *Polymer Degradation and Stability*, 95(12):2584–2588, 2010.

- [54] Jianxiong Ni, Lijuan Chen, Kuiming Zhao, Yuan Hu, and Lei Song. Preparation of gel-silica/ammonium polyphosphate core-shell flame retardant and properties of polyurethane composites. *Polymers for Advanced Technologies*, 22(12):1824–1831, 2011.
- [55] Hongqiang Qu, Weihong Wu, Jianwei Hao, Chunzheng Wang, and Jianzhong Xu. Inorganic–organic hybrid coating-encapsulated ammonium polyphosphate and its flame retardancy and water resistance in epoxy resin. *Fire and Materials*, 38(3):312–322, 2014.
- [56] Thomas Fütterer, Hans-Dieter Naegerl, Vincens Mans Fibia, and Siegfried Mengel. Flame-proofed polymer material, May 21 2013. US Patent 8,444,884.
- [57] Pin Lv, Zhengzhou Wang, Keliang Hu, and Weicheng Fan. Flammability and thermal degradation of flame retarded polypropylene composites containing melamine phosphate and pentaerythritol derivatives. *Polymer Degradation and Stability*, 90(3):523–534, 2005.
- [58] Yinghong Chen and Qi Wang. Reaction of melamine phosphate with pentaerythritol and its products for flame retardation of polypropylene. *Polymers for Advanced Technologies*, 18(8):587–600, 2007.
- [59] Shun Zhou, Zhengzhou Wang, Zhou Gui, and Yuan Hu. Flame retardation and thermal degradation of flame-retarded polypropylene composites containing melamine phosphate and pentaerythritol phosphate. *Fire and materials*, 32(5):307–319, 2008.
- [60] Gousheng Liu, Wenyan Chen, and Jianguo Yu. A novel process to prepare ammonium polyphosphate with crystalline form ii and its comparison with melamine polyphosphate. *Industrial & Engineering Chemistry Research*, 49(23):12148–12155, 2010.
- [61] SV Levchik, AI Balabanovich, GF Levchik, and L Costa. Effect of melamine and its salts on combustion and thermal decomposition of polyamide 6. *Fire and Materials*, 21(2):75–83, 1997.
- [62] Yinghong Chen and Qi Wang. Preparation, properties and characterizations of halogen-free nitrogen–phosphorous flame-retarded glass fiber reinforced polyamide 6 composite. *Polymer degradation and stability*, 91(9):2003–2013, 2006.
- [63] Yi Xu, Yuan Liu, and Qi Wang. Melamine polyphosphate/silicon-modified phenolic resin flame retardant glass fiber reinforced polyamide-6. *Journal of Applied Polymer Science*, 129(4):2171–2176, 2013.
- [64] P Kiliaris, CD Papaspyrides, R Xalter, and R Pfaendner. Study on the properties of polyamide 6 blended with melamine polyphosphate and layered silicates. *Polymer degradation and stability*, 97(7):1215–1222, 2012.

- [65] Qilong Tai, Richard KK Yuen, Wei Yang, Zhihua Qiao, Lei Song, and Yuan Hu. Iron-montmorillonite and zinc borate as synergistic agents in flame-retardant glass fiber reinforced polyamide 6 composites in combination with melamine polyphosphate. *Composites Part A: Applied Science and Manufacturing*, 43(3):415–422, 2012.
- [66] Anna Hermansson, Thomas Hjertberg, and Bernt-Åke Sultan. Distribution of calcium carbonate and silicone elastomer in a flame retardant system based on ethylene-acrylate copolymer, chalk and silicone elastomer and its effect on flame retardant properties. *Journal of applied polymer science*, 100(3):2085–2095, 2006.
- [67] Anna Hermansson, Thomas Hjertberg, and Bernt-Åke Sultan. Linking the flame-retardant mechanisms of an ethylene-acrylate copolymer, chalk and silicone elastomer system with its intumescent behaviour. *Fire and materials*, 29(6):407–423, 2005.
- [68] Anna Hermansson, Thomas Hjertberg, and Bernt-Åke Sultan. The flame retardant mechanism of polyolefins modified with chalk and silicone elastomer. *Fire and materials*, 27(2):51–70, 2003.
- [69] JL Shotwell, ME Razzoog, and A Koran. Color stability of long-term soft denture liners. *The Journal of prosthetic dentistry*, 68(5):836–838, 1992.
- [70] Anthony Davis and David Sims. *Weathering of polymers*. Springer Science & Business Media, 1983.
- [71] JR White and A Turnbull. Weathering of polymers: mechanisms of degradation and stabilization, testing strategies and modelling. *Journal of materials science*, 29(3):584–613, 1994.
- [72] Roger L Clough and Kenneth T Gillen. Combined environment aging effects: Radiation-thermal degradation of polyvinylchloride and polyethylene. *Journal of Polymer Science: Polymer Chemistry Edition*, 19(8):2041–2051, 1981.
- [73] NC Billingham. Developments in polymer stabilisation—6: Edited by g. scott, applied science publishers ltd. 1983. price:£ 40. 00, 1984.
- [74] BB Troitskii and LS Troitskaya. The mathematical models of the initial stage of the thermal degradation of poly (vinyl chloride). *International Journal of Polymeric Materials*, 13(1-4):169–178, 1990.
- [75] MWA Paterson and JR White. Effect of water absorption on residual stresses in injection-moulded nylon 6, 6. *Journal of materials science*, 27(22):6229–6240, 1992.
- [76] David P Garner, G Allen Stahl, et al. *Effects of hostile environments on coatings and plastics*. American Chemical Society, 1983.

- [77] Gerald Scott. Mechano-chemical degradation and stabilization of polymers. *Polymer Engineering & Science*, 24(13):1007–1020, 1984.
- [78] Anatoliĭ Popov. *Oxidation of stressed polymers*.
- [79] AA Popov, BE Krysyuk, and GY Zaikow. Translation of vysokomol soyed. *Polymer science USSR*, 22, 1980.
- [80] AA Popov, BE Krisyuk, NN Blinov, and GE Zaikov. On the effect of stress on oxidative destruction of polymers. the action of ozone on polyolefines. *European Polymer Journal*, 17(2):169–173, 1981.
- [81] NM Livanova, N Ya Rapoport, and G Ye Zaikov. Focal character of oxidation and the scale effect in the longevity of oriented polypropylene. *Polymer Science USSR*, 30(8):1734–1741, 1988.
- [82] SN Zhurkov, VA Zakrevskiy, VE Korsukov, and VS Kuksenko. Mechanism of submicrocrack generation in stressed polymers. *Journal of Polymer Science Part A-2: Polymer Physics*, 10(8):1509–1520, 1972.
- [83] F Bueche. Tensile strength of plastics above the glass temperature. *Journal of Applied Physics*, 26(9):1133–1140, 1955.
- [84] MM Qayyum and JR White. Effect of water absorption and temperature gradients on polycarbonate injection moldings. *Journal of applied polymer science*, 43(1):129–144, 1991.
- [85] C T KELLY, Li Tong, and JR White. Slow strain-rate testing of polymers with ultraviolet exposure. *Journal of materials science*, 32(4):851–861, 1997.
- [86] DP Russell and Peter WR Beaumont. Structure and properties of injection-molded nylon-6. 2. residual-stresses in injection-molded nylon-6. *Journal of Materials Science*, 15(1):208–215, 1980.
- [87] MWA Paterson and JR White. Layer removal analysis of residual stress. *Journal of materials science*, 24(10):3521–3528, 1989.
- [88] A Blaga. Weathering study of glass-fiber reinforced polyester sheets by scanning electron microscopy. *Polymer Engineering & Science*, 12(1):53–58, 1972.
- [89] JR White. Effect of secondary crystallization on residual stresses in moulded polymers. *Journal of materials science letters*, 9(1):100–101, 1990.
- [90] A Siegmann and S Kenig. Simultaneous residual stresses and crystallinity changes during ageing of polyoxymethylene. *Journal of materials science letters*, 5(12):1213–1215, 1986.
- [91] P Komitov, G Kostov, and S Stanchev. Ageing of ldpe: Structural changes. *Polymer degradation and stability*, 24(4):303–312, 1989.

- [92] Xavier Almeras, Michel Le Bras, Peter Hornsby, Serge Bourbigot, Gyorgy Marosi, Peter Anna, and René Delobel. Artificial weathering and recycling effect on intumescent polypropylenebased blends. *Journal of fire sciences*, 22(2):143–161, 2004.
- [93] Sami Ullah, Faiz Ahmad, AM Shariff, and MA Bustam. Synergistic effects of kaolin clay on intumescent fire retardant coating composition for fire protection of structural steel substrate. *Polymer Degradation and Stability*, 110:91–103, 2014.
- [94] Ulrike Braun, Volker Wachtendorf, Anja Geburtig, Horst Bahr, and Bernhard Schartel. Weathering resistance of halogen-free flame retardance in thermoplastics. *Polymer Degradation and Stability*, 95(12):2421–2429, 2010.
- [95] Toshiro Harada, Yasushi Nakashima, and Yasushi Anazawa. The effect of ceramic coating of fire-retardant wood on combustibility and weatherability. *Journal of Wood Science*, 53(3):249–254, 2007.
- [96] Xavier Almeras, Michel Le Bras, Peter Hornsby, Serge Bourbigot, Gyorgy Marosi, Peter Anna, and René Delobel. Artificial weathering and recycling effect on intumescent polypropylenebased blends. *Journal of fire sciences*, 22(2):143–161, 2004.
- [97] TA Roberts, LC Shirvill, K Waterton, and I Buckland. Fire resistance of passive fire protection coatings after long-term weathering. *Process Safety and Environmental Protection*, 88(1):1–19, 2010.
- [98] Annette Naumann, Henrik Seefeldt, Ina Stephan, Ulrike Braun, and Matthias Noll. Material resistance of flame retarded wood-plastic composites against fire and fungal decay. *Polymer degradation and stability*, 97(7):1189–1196, 2012.
- [99] Sahotra Sarkar. Evolutionary theory in the 1920s: the nature of the “synthesis”. *Philosophy of Science*, 71(5):1215–1226, 2004.
- [100] Robert R Pagano. *Understanding statistics in the behavioral sciences*. Cengage Learning, 2012.
- [101] Xavier Silvani and Frédéric Morandini. Fire spread experiments in the field: temperature and heat fluxes measurements. *Fire Safety Journal*, 44(2):279–285, 2009.
- [102] Mark McKinnon. Cone calorimetry.
- [103] Clayton Huggett. Estimation of rate of heat release by means of oxygen consumption measurements. *Fire and Materials*, 4(2):61–65, 1980.
- [104] Vytenis Babrauskas. *Heat release in fires*. Taylor & Francis, 1990.
- [105] Vytenis Babrauskas. *Ignition handbook*, volume 98027. Fire Science Publishers,

Issaquah, WA, 2003.

- [106] Geoffrey Cox and Brian Langford. *Fire Safety Science: Proceedings of the Third International Symposium*. Taylor & Francis, 1991.
- [107] Marc Janssens. *Fundamental thermophysical characteristics of wood and their role in enclosure fire growth*. PhD thesis, Ghent University, 1991.
- [108] Takayuki Fueno. *Transition State: A Theoretical Approach*. CRC Press, 1999.
- [109] SJ Melinek. Ignition behaviour of heated wood surfaces. *Fire Safety Science*, 755:1–1, 1969.

APPENDIX: RAW DATA

The combustion properties measured by cone calorimeter are presented in this Appendix. I have to thank Babak Bahrani who measured these data after long hours of laboratory working and shared generously the results. Based on MANOVA results, the orientation of installation can be removed from the list of effective treatments. This point provides statistical permission to combine the data from Northward and Southward installed samples on the weathering fence together. After this process, most of the classes contain 6 members rather than 3. However, the first three data in each cell came from the northward installation of the samples on the fence.

LOW HEAT FLUX (TTI)				
	Type A	Type B	Type C	Uncoated
0-Month	305	515	415	71
	260	355	201	78
	355	402	335	88
Mean	306.6667	424.0000	317.0000	79.0000
St. D.	42.5049	73.5554	96.7140	7.6420
3-Month	121	66	348	26
	130	66	125	31
	76	66	277	29
	114	82	166	39
	122	73	199	36
	78	63	231	38
Mean	106.8333	69.3333	224.3333	33.1667
St. D.	23.6678	7.0333	80.0292	5.2694
6-Month	104	83	291	65
	135	85	234	33
	119	79	241	82
	105	61	161	46
	96	55	211	40
	132	68	261	77
Mean	115.1667	71.8333	233.1667	57.1667
St. D.	16.0427	12.3680	44.4541	20.3707
12-Month	50	88	627	26
	93	62	627	64
	65	48	627	40
	89	45	175	65
	61	64	285	27
	71	59	153	37
Mean	71.5000	61.0000	415.6667	43.1667
St. D.	16.6343	15.2840	235.7852	17.4059

MEDIUM HEAT FLUX (TTI)				
	Type A	Type B	Type C	Uncoated
0-Month	58	31	171	18
	64	21	339	21
	85	27	366	20
Mean	69.0000	26.3333	292.0000	19.6667
St. D.	12.6807	4.5019	94.5008	1.3663
3-Month	22	44	28	12
	34	34	27	15
	32	48	90	14
	21	12	50	6
	27	15	39	13
	35	26	28	10
Mean	28.5000	29.8333	43.6667	11.6667
St. D.	6.0910	14.8380	24.4022	3.2660
6-Month	21	24	24	17
	36	15	41	15
	61	14	70	16
	46	34	30	15
	23	30	34	17
	40	28	38	8
Mean	37.8333	24.1667	39.5000	14.6667
St. D.	14.9321	8.1588	16.0966	3.3862
12-Month	44	17	55	11
	16	19	34	10
	26	14	133	9
	33	19	89	11
	36	14	29	6
	23	19	24	6
Mean	29.6667	17.0000	60.6667	8.8333
St. D.	10.0133	2.4495	42.7208	2.3166

HIGH HEAT FLUX (TTI)				
	Type A	Type B	Type C	Uncoated
0-Month	45	20	23	11
	30	17	13	8
	42	18	20	10
Mean	39.0000	18.3333	18.6667	9.6667
St. D.	7.0993	1.3663	4.5898	1.3663
3-Month	20	9	11	4
	17	13	13	7
	15	12	16	6
	17	21	12	3
	15	13	16	5
	16	14	14	4
Mean	16.6667	13.6667	13.6667	4.8333
St. D.	1.8619	3.9833	2.0656	1.4720
6-Month	23	18	12	8
	29	17	40	6
	28	12	31	6
	20	17	21	7
	23	16	13	8
	14	14	22	6
Mean	22.8333	15.6667	23.1667	6.8333
St. D.	5.4924	2.2509	10.7595	0.9832
12-Month	25	11	11	6
	7	14	18	6
	27	8	14	6
	19	7	14	6
	16	8	9	7
	20	6	13	8
Mean	19.0000	9.0000	13.1667	6.5000
St. D.	7.1274	2.9665	3.0605	0.8367

LOW HEAT FLUX (HRR)				
	Type A	Type B	Type C	Uncoated
0-Month	76.6900	53.6800	31.0600	113.5200
	47.0500	106.5700	44.0500	112.0000
	78.9800	77.1900	78.9700	101.6200
Mean	67.5733	79.1467	51.3600	109.0467
St. D.	15.9303	23.7016	22.1616	5.7927
3-Month	102.5700	97.6500	36.4200	102.0000
	66.8100	89.5000	33.0500	103.0000
	76.1100	93.5750	42.5100	101.0000
	51.9100	97.3800	34.8900	106.3300
	49.0500	107.4000	29.0000	103.6300
	50.2300	95.6900	21.0600	105.0000
Mean	66.1133	96.8658	32.8217	103.4933
St. D.	20.8551	5.9719	7.2675	1.9507
6-Month	80.3900	72.3200	28.0700	125.3900
	58.5600	84.7800	18.2600	100.5300
	55.8100	101.2900	44.8100	150.3700
	55.8400	103.0700	40.1800	115.7000
	49.6800	98.9000	27.0000	106.6400
	78.1700	87.9300	13.8400	136.4500
Mean	63.0750	91.3817	28.6933	122.5133
St. D.	12.9043	11.9177	12.0368	18.7625
12-Month	76.2700	124.1100	9.0000	93.1600
	95.9700	98.0000	9.6800	107.2400
	87.0000	118.0000	11.0000	93.4900
	106.7500	105.1000	48.0800	102.8800
	85.9800	117.6000	30.9700	88.9200
	98.0000	119.4900	40.0000	85.5300
Mean	91.6617	113.7167	24.7883	95.2033
St. D.	10.7453	9.9603	17.2033	8.2943

MEDUIM HEAT FLUX (HRR)				
	Type A	Type B	Type C	Uncoated
0-Month	87.7300	76.5900	58.7600	172.3300
	74.5600	58.5000	127.9000	137.8900
	114.3900	67.1800	56.4200	175.4700
Mean	92.2267	67.4233	81.0267	161.8967
St. D.	18.1499	8.0923	36.3230	18.6484
3-Month	123.5400	171.7100	10.8300	183.2500
	143.0900	109.2400	11.1800	202.7900
	140.5100	180.0100	45.0400	193.0000
	151.5500	120.7800	57.1700	177.5000
	120.0000	100.6900	11.1500	170.3500
	143.9900	166.7100	12.1500	174.0000
Mean	137.1133	141.5233	24.5867	183.4817
St. D.	12.4905	35.1189	20.9008	12.3417
6-Month	107.9300	88.3300	14.1300	159.3200
	125.9400	89.3800	10.3300	175.2900
	115.4700	122.3500	43.4300	171.1800
	105.3700	144.9800	14.7500	171.0500
	90.5400	143.2100	9.9900	179.4800
	108.3300	128.5300	16.2000	155.8900
Mean	108.9300	119.4633	18.1383	168.7017
St. D.	11.6990	25.2184	12.6360	9.2021
12-Month	134.8700	149.9500	39.7600	156.5100
	142.4100	143.0000	55.0000	187.1100
	149.0300	147.0000	46.1000	153.2300
	119.9000	159.7100	10.0100	149.3200
	145.4900	171.0400	10.8600	146.9900
	109.3200	152.3500	13.7700	153.3700
Mean	133.5033	153.8417	29.2500	157.7550
St. D.	15.7216	10.1187	20.0272	14.7649

HIGH HEAT FLUX (HRR)				
	Type A	Type B	Type C	Uncoated
0-Month	120.8600	80.4300	38.0000	183.0100
	119.7200	66.6200	44.5200	168.4400
	167.9000	103.1900	61.5200	233.2700
Mean	136.1600	83.4133	48.0133	194.9067
St. D.	24.5910	16.5171	10.8609	30.4221
3-Month	112.6800	120.4300	24.5300	171.3400
	157.1800	199.3800	69.3700	219.0400
	157.0900	162.0300	28.8300	195.0000
	78.1800	225.3900	40.6800	224.9200
	175.4600	189.0300	43.6200	262.0500
	166.7300	161.5000	29.3600	243.0000
Mean	141.2200	176.2933	39.3983	219.2250
St. D.	37.7314	36.4656	16.4395	32.5930
6-Month	89.7000	187.4900	22.2500	234.7700
	136.8700	171.0100	49.7100	260.0500
	220.8900	153.6800	58.1100	234.4700
	114.6900	155.3000	32.9900	208.7100
	164.6800	168.2900	18.8100	219.8900
	151.6200	178.6700	68.0400	187.5100
Mean	146.4083	169.0733	41.6517	224.2333
St. D.	45.2137	13.1324	20.0267	24.9282
12-Month	182.0000	218.1800	38.2100	257.1200
	198.0000	203.7600	25.0000	238.0000
	235.0900	200.1000	36.5000	267.4100
	207.4400	197.8300	28.0000	256.2300
	198.2600	230.7000	56.0000	270.3200
	202.3600	223.3300	67.0000	267.9600
Mean	203.8583	212.3167	41.7850	259.5067
St. D.	17.5154	13.6084	16.4337	12.0815

LOW HEAT FLUX (MLR)				
	Type A	Type B	Type C	Uncoated
0-Month	7.8300	7.3400	5.5800	12.5800
	7.3400	9.4700	5.5600	9.4000
	6.8400	7.4700	5.1900	10.0200
Mean	7.3367	8.0933	5.4433	10.6667
St. D.	0.4427	1.0679	0.1964	1.5078
3-Month	11.3900	10.6400	7.3800	12.2200
	9.8100	9.3500	7.8100	14.7300
	10.1300	10.0000	7.0800	13.5000
	9.7200	9.8400	8.3100	9.3900
	9.0800	10.4200	3.0700	11.5600
	8.4200	9.3000	3.3900	10.5000
Mean	9.7583	9.9250	6.1733	11.9833
St. D.	1.0056	0.5460	2.3195	1.9496
6-Month	7.8300	4.6700	7.1200	13.3800
	8.6600	6.2200	8.0200	12.2000
	9.4700	6.8900	8.2700	14.9200
	8.2200	8.2900	7.4400	14.0400
	8.9800	9.6400	3.0700	10.7900
	8.9200	9.5200	4.3300	12.2100
Mean	8.6800	7.5383	6.3750	12.9233
St. D.	0.5842	1.9644	2.1490	1.4849
12-Month	10.0700	14.3300	4.4600	11.8600
	11.8700	11.2000	4.9800	12.7700
	12.1800	12.4200	6.3000	12.8900
	12.0700	9.8800	7.4500	12.4400
	12.0800	10.8100	7.6400	12.1600
	11.9800	11.2200	3.7000	13.2500
Mean	11.7083	11.6433	5.7550	12.5617
St. D.	0.8094	1.5493	1.6263	0.5086

MEDUIM HEAT FLUX (MLR)				
	Type A	Type B	Type C	Uncoated
0-Month	11.0500	7.7500	10.2800	16.5100
	12.6100	8.5700	15.1800	15.7200
	4.7300	12.4400	9.7200	18.6200
Mean	9.4633	9.5867	11.7267	16.9500
St. D.	3.7322	2.2404	2.6866	1.3410
3-Month	13.0100	15.2900	10.0400	19.0900
	14.7200	10.6900	9.7700	19.4700
	16.0000	8.8100	10.9300	19.3000
	14.6400	15.2200	11.8700	16.6200
	13.3300	13.3000	9.7800	19.3400
	14.0200	15.6500	10.5500	18.0000
Mean	14.2867	13.1600	10.4900	18.6367
St. D.	1.0830	2.8293	0.8157	1.1231
6-Month	12.8200	10.4400	7.0600	20.3000
	13.8700	10.6000	9.0600	19.0700
	12.9800	14.4500	10.4500	19.1800
	9.8200	15.9200	4.1800	20.0500
	11.8300	13.1700	5.1400	18.7300
	11.6000	14.8800	8.3900	20.2400
Mean	12.1533	13.2433	7.3800	19.5950
St. D.	1.4093	2.2869	2.3928	0.6806
12-Month	15.6500	17.0200	13.2400	17.8500
	16.1500	15.9100	10.6400	19.9500
	16.7300	16.8500	9.0000	17.7200
	13.1600	17.5800	9.4400	13.5300
	14.4300	19.3100	8.7700	15.3400
	13.9900	17.6000	8.4800	16.4700
Mean	15.0183	17.3783	9.9283	16.8100
St. D.	1.3760	1.1300	1.7896	2.2273

HIGH HEAT FLUX (MLR)				
	Type A	Type B	Type C	Uncoated
0-Month	5.2100	12.1900	4.9953	16.7000
	4.2600	11.8800	10.4900	15.7800
	5.0100	10.3500	10.9000	21.5200
Mean	4.8267	11.4733	8.7951	18.0000
St. D.	0.4480	0.8811	2.9490	2.7574
3-Month	6.0100	11.7400	12.2900	15.8900
	5.1500	19.2400	12.5200	19.2200
	18.2200	17.0300	10.9500	17.7000
	4.1900	21.5800	11.1700	21.7300
	18.9800	17.7900	10.1500	22.8400
	4.6500	16.6900	9.4900	22.3000
Mean	9.5333	17.3450	11.0950	19.9467
St. D.	7.0530	3.2762	1.1794	2.7972
6-Month	16.1000	18.2800	10.0200	23.2400
	16.0600	16.6400	10.4100	25.4100
	21.6900	18.4600	11.3600	24.9100
	15.6000	16.7700	11.5100	21.8200
	19.0500	17.9200	11.7500	23.4500
	18.1000	17.9100	13.4300	16.5800
Mean	17.7667	17.6633	11.4133	22.5683
St. D.	2.3467	0.7729	1.1950	3.2002
12-Month	16.3300	19.9700	13.5800	23.7200
	20.4100	18.7100	8.7100	22.9200
	18.7700	17.7000	11.1500	24.1500
	21.2200	20.9800	10.9900	23.7200
	19.2400	22.6000	13.9500	24.2000
	20.9600	22.6300	14.7600	25.3900
Mean	19.4883	20.4317	12.1900	24.0167
St. D.	1.8203	2.0236	2.2920	0.8144

LOW HEAT FLUX (EHC)				
	Type A	Type B	Type C	Uncoated
0-Month	13.6700	14.2300	15.0200	13.3600
	13.3100	17.9200	13.7400	10.8700
	20.8200	15.4500	13.7300	12.6300
Mean	15.9333	15.8667	14.1633	12.2867
St. D.	3.7886	1.6815	0.6636	1.1449
3-Month	12.4400	12.8300	12.0400	10.4000
	11.2300	13.0000	11.5700	11.4000
	12.1400	12.9000	12.2500	9.4000
	11.3100	13.5900	10.2400	11.7400
	12.5100	13.4100	10.2000	10.7200
	11.3600	13.4800	4.4000	11.2000
Mean	11.8317	13.2017	10.1167	10.8100
St. D.	0.5970	0.3291	2.9348	0.8402
6-Month	11.7500	17.0600	12.7100	11.4100
	11.9100	18.1500	10.9100	11.1800
	11.5200	17.1100	11.8700	11.0500
	11.5700	16.7900	12.0200	11.1200
	10.4300	12.1300	12.0000	11.1800
	12.3600	12.0800	5.3200	11.2400
Mean	11.5900	15.5533	10.8050	11.1967
St. D.	0.6437	2.7110	2.7482	0.1227
12-Month	11.6700	11.7100	1.6400	10.0700
	11.3900	10.6500	2.0800	10.0100
	7.8500	11.1900	1.5100	9.8800
	12.0600	10.9500	10.3100	10.1700
	11.2300	11.2600	10.3800	9.5900
	11.7400	11.2900	0.9600	9.6100
Mean	10.9900	11.1750	4.4800	9.8883
St. D.	1.5651	0.3559	4.5571	0.2424

MEDIUM HEAT FLUX (EHC)				
	Type A	Type B	Type C	Uncoated
0-Month	12.1300	11.9600	11.5700	14.0600
	13.0700	13.1900	13.6900	13.0000
	14.2200	12.8900	11.2100	13.0600
Mean	13.1400	12.6800	12.1567	13.3733
St. D.	0.9362	0.5736	1.1986	0.5326
3-Month	14.1900	15.8200	8.8800	12.5700
	13.2900	21.1700	9.7900	13.1800
	13.9200	25.7600	12.3300	12.9000
	13.8400	12.6800	12.6200	12.4900
	13.5300	21.9600	10.5200	12.0500
	13.7600	12.8700	9.2300	12.3000
Mean	13.7550	18.3767	10.5617	12.5817
St. D.	0.3132	5.3753	1.5851	0.4074
6-Month	13.6800	12.8100	1.4800	11.2500
	12.1200	11.8500	7.8000	11.7800
	12.9800	12.6000	11.7900	11.6800
	13.8500	12.3900	3.4000	11.5700
	13.6800	12.2300	2.5200	12.3000
	11.5300	12.6000	7.8200	11.2600
Mean	12.9733	12.4133	5.8017	11.6400
St. D.	0.9569	0.3402	3.9785	0.3894
12-Month	11.9300	11.8200	10.2400	12.1600
	12.1000	11.4200	11.4100	13.0900
	11.8300	11.5100	10.7800	12.2500
	11.5900	11.3200	8.1500	11.6800
	12.0600	11.6000	10.5200	11.6000
	11.3300	11.3000	7.4300	11.9900
Mean	11.8067	11.4950	9.7550	12.1283
St. D.	0.2967	0.1955	1.5869	0.5366

HIGH HEAT FLUX (EHC)				
	Type A	Type B	Type C	Uncoated
0-Month	17.1000	12.6900	12.9100	12.9100
	19.6500	12.9900	12.5900	13.8300
	18.3900	13.7300	12.1000	13.3300
Mean	18.3800	13.1367	12.5333	13.3567
St. D.	1.1404	0.4788	0.3649	0.4120
3-Month	16.3200	10.4300	10.6100	12.0400
	23.3100	12.4000	12.3700	12.7800
	12.2000	12.3400	11.8200	12.4000
	15.8900	12.9700	11.9400	12.6500
	12.8400	10.5600	11.7700	13.0600
	19.4000	12.7600	11.4900	12.9000
Mean	16.6600	11.9100	11.6667	12.6383
St. D.	4.1695	1.1211	0.5918	0.3691
6-Month	11.5700	12.5100	10.5100	11.8200
	12.0700	12.3700	12.3000	11.8300
	12.8400	12.6500	11.8900	11.4800
	12.3100	12.2400	11.0600	11.3300
	12.4400	12.8900	10.7300	11.7000
	11.9900	12.6200	12.1900	11.4900
Mean	12.2033	12.5467	11.4467	11.6083
St. D.	0.4329	0.2283	0.7769	0.2051
12-Month	11.8800	11.7700	10.8800	12.6700
	11.8500	12.2700	9.8400	12.6500
	14.4200	11.7800	10.3800	12.8200
	12.6300	12.0000	10.4300	13.0300
	12.3100	12.5300	11.5000	13.2400
	12.0800	12.1600	11.0600	12.9300
Mean	12.5283	12.0850	10.6817	12.8900
St. D.	0.9714	0.2958	0.5856	0.2257